TABLE 1
Replication of viruses from the HIV-1 V3 loop library in PM1 and PM1/CCR5 cells

Viral clone	V3 sequence	p24 Gag antigen (ng/ml)[a]		
		PM1	PM1/CCR5	Ratio[b]
$HIV\text{-}1_{JR\text{-}FLan}$	CTRPNNNTRKSIHIGPGRAFYTTGEIIGDIRQAHC	140	270	1.9
#01	.....RG.PM.....HV.....	18	50	2.8
#02	.....L.....L.A..D...N.....	17	54	3.2
#03	.....RG.PL.....C.A..AV.....	<1.0	<1.0	–
#04	.....RGVYL.....PV.....	<1.0	<1.0	–
#05	.....R..NL.....L.....V..N.....	70	49	0.7
#06	.....R.VS.....L.A...V..N.....	46	17	0.4
#07	.....RG.PM.....W.A..H.....	23	20	0.9
#08	.....VTM.....L.A..DV..N.....	83	8.0	0.1
#09	.....GVNL.....L.A..DV.....	51	20	0.4
#10	.....S.....A..HV..N.....	21	220	10
#11	.....RGV.L.....PV.....	<1.0	<1.0	–
#12	.....VN.....A..PI..N.....	<1.0	<1.0	–
#13	.....R.VNL.....W....Q.....	4.0	5.0	1.3
#14	.....RGVPL.....A.....	<1.0	<1.0	–
#15	.....G..L.....C....H...N.....	<1.0	<1.0	–
#16	.....RG.YM.....L....QV.....	6.0	160	27
#17	.....RGVPL.....A..DV..N.....	3.0	10	3.3
#18	.....YL.....L....P...N.....	<1.0	<1.0	–
#19	.....GVT.....W.A.....	38	29	0.8
#20	.....RGVYM.....C....A...N.....	<1.0	<1.0	–
#21	.....NL.....Q...N.....	7.0	140	20
#22	.....VPM.....A.VAV..N.....	5.0	53	11
#23	.....VNM.....L....D.....	120	14	0.1
#24	.....R.VPL.....W.A.....N.....	3.0	3.0	1.0
#25	.....R.V.M.....V..N.....	70	6.0	0.1
#26	.....GVTL.....L.....V.....	<1.0	<1.0	–
#27	.....GVNL.....L.....V.....	13	8.0	0.6
#28	.....G.PL.....L.A..HV..N.....	40	47	1.2
#29	.....RG.PM.....PV..N.....	7.0	100	27
#30	.....SM.....W.A..P...N.....	2.0	2.0	1.0
#31	.....L.....C....H...N.....	<1.0	<1.0	–
#32	.....RG..L.....L.....N.....	3.0	3.0	1.0
#33	.....T.....W....PV..N.....	3.0	5.0	1.7
#34	.....GVYM.....L.S..D.....	7.0	170	24
#35	.....RGV.L.....W.A..H...N.....	2.0	2.0	1.0
#36	.....RG.....H.....	3.0	3.0	1.0
#37	.....TM.....L.A..P...N.....	<1.0	<1.0	–
#38	.....G.Y.....D.....	3.0	23	7.7
#39	.....Y.....P.....	5.0	37	7.4
#40	.....RG.TL.....W.A.....	<1.0	<1.0	–
#41	.....G..M.....C....PV..N.....	<1.0	<1.0	–
#42	.....RG.....L.A..PV..N.....	<1.0	<1.0	–
#43	.....L.....L.A..PV.....	60	24	0.4
#44	.....VP.....C.A..A...N.....	<1.0	<1.0	–
#45	.....RGET.....L....AV..N.....	<1.0	<1.0	–

[a] PM1 or PM1/CCR5 cells (4 10^4) were infected with each virus (8 ng of p24 Gag). On day 6 the extent of viral replication was measured by p24 Gag ELISA. Results represent the average of three independent experiments.
[b] Ratio, the concentration of p24 Gag in the supernatant of PM1/CCR5 cells was divided by that of PM1 cells.

(TAK-779) to block secondary infection by nascent progeny virus. The concentrations of AZT and TAK-779 used were 4 and 1 M, respectively, 78- and 32-fold higher than the respective IC_{50} levels (the concentration required to inhibit 50% of the blue foci formation in MAGIC5 cells) (data not shown). Note that on day 2 post-infection, the number of viruses generated from

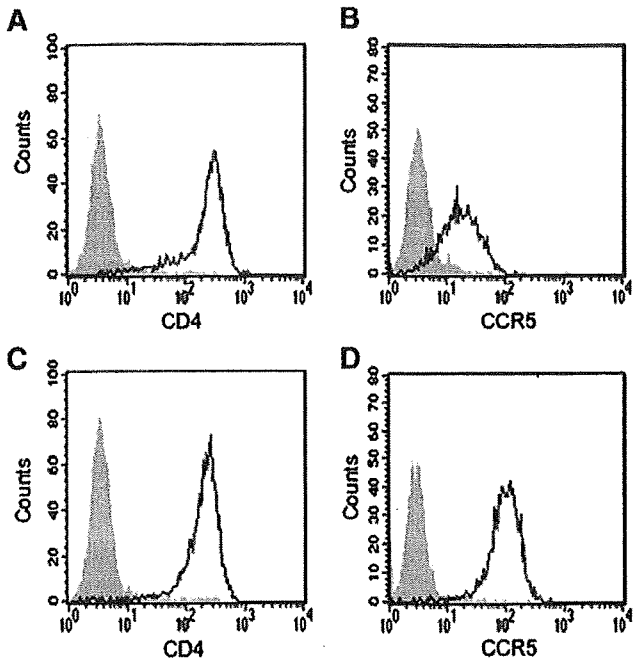

FIGURE 2. **Expression of CD4 and CCR5 in PM1 and PM1/CCR5 cells.** The cells were stained with mAb directed against CD4 (SK3) or CCR5 (2D7) and analyzed by flow cytometry. *A*, CD4 in PM1 cells. *B*, CCR5 in PM1 cells. *C*, CD4 in PM1/CCR5 cells; *D*, CCR5 in PM1/CCR5 cells. The *shaded histograms* indicate background staining with secondary antibody alone. The *open histograms* represent staining with indicated primary antibody.

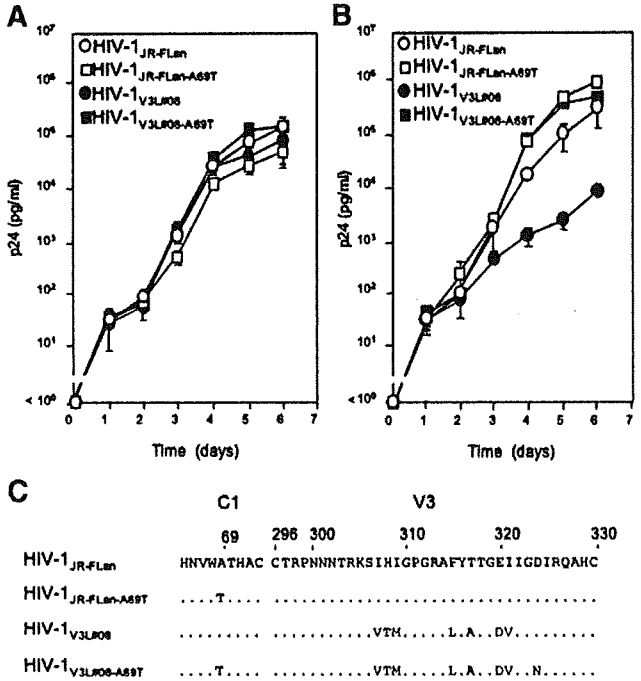

FIGURE 3. **Suppression of HIV-$1_{V3L\#08}$ replication in PM1/CCR5 cells.** Replication kinetics of HIV-$1_{JR\text{-}FLan}$, HIV-$1_{JR\text{-}FLan\text{-}A69T}$, HIV-$1_{V3L\#08}$, and HIV-$1_{V3L\#08\text{-}A69T}$ in PM1 cells (*A*) and in PM1/CCR5 cells (*B*). Cells (4 10^4) were infected with 8 ng of p24 Gag. Viral replication was monitored by measuring p24 Gag production. *C*, amino acid substitutions in the gp120 V3 loop and C1 of HIV-$1_{JR\text{-}FLan}$, HIV-$1_{JR\text{-}FLan\text{-}A69T}$, HIV-$1_{V3L\#08}$, and HIV-$1_{V3L\#08\text{-}A69T}$. The analysis was repeated three times; *error bars* represent S.D. of three replicates.

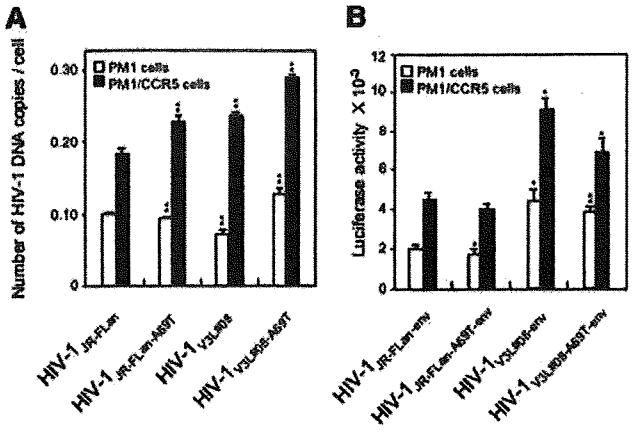

FIGURE 4. **Entry of HIV-$1_{JR\text{-}FLan}$, HIV-$1_{JR\text{-}FLan\text{-}A69T}$, HIV-$1_{V3L\#08}$, and HIV-$1_{V3L\#08\text{-}A69T}$ into PM1 or PM1/CCR5 cells.** *A*, PM1 and PM1/CCR5 cells were infected with 30 ng of p24 HIV-1 for 2 h. Eight hours after infection, synthesized proviral HIV-1 DNA was determined by *TaqMan* real-time PCR. *B*, PM1 or PM1/CCR5 cells were infected for 2 h with viruses pseudotyped with the envelope of HIV-$1_{JR\text{-}FLan}$, HIV-$1_{JR\text{-}FLan\text{-}A69T}$, HIV-$1_{V3L\#08}$, or HIV-$1_{V3L\#08\text{-}A69T}$ (8 ng of p24 Gag). At 48 h post-infection, luciferase activity in cell lysate was determined. The analysis was repeated three times; *error bars* represent the S.D. of three replicates. *, p 0.01; **, p 0.001. Statistical significant differences were calculated by *t* test *versus* HIV-$1_{JR\text{-}FLan}$.

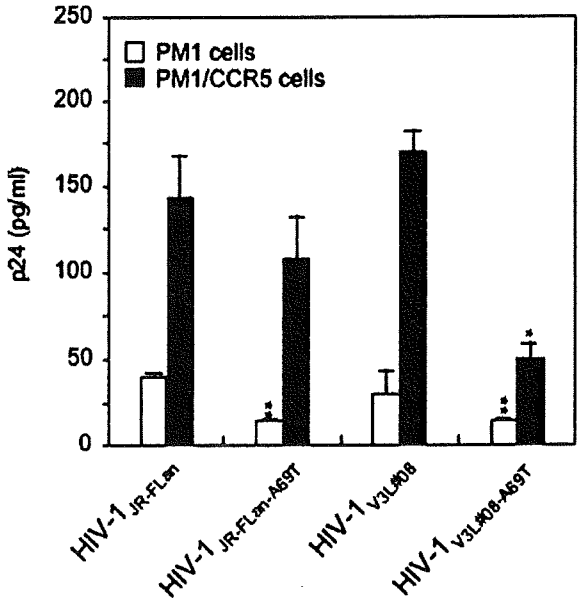

FIGURE 5. **Production of HIV-$1_{JR\text{-}FLan}$, HIV-$1_{JR\text{-}FLan\text{-}A69T}$, HIV-$1_{V3L\#08}$, and HIV-$1_{V3L\#08\text{-}A69T}$ from PM1 or PM1/CCR5 cells in the presence of AZT and TAK-779.** The cells were infected with each virus (8 ng of p24 Gag) for 2 h, then 1 M AZT and 4 M TAK779 were added. On day 2, the level of p24 Gag in the supernatant was determined by p24 Gag ELISA. The analysis was repeated three times; *error bars* represent the S.D. of three replicates. *, p 0.01; **, p 0.001. Statistical significant differences were calculated by *t* test *versus* HIV-$1_{JR\text{-}FLan}$.

HIV-$1_{V3L\#08}$-infected PM1/CCR5 cells was 5.7-fold higher than PM1-infected cells (Fig. 5). HIV-$1_{JR\text{-}FLan}$, HIV-$1_{JR\text{-}FLan\text{-}A69T}$, HIV-$1_{V3L\#08}$, and HIV-$1_{V3L\#08\text{-}A69T}$ showed similar results. Production of these viruses generated from PM1/CCR5 cells was 3.8–8.7-fold higher than from PM1 cells, demonstrating that V3 loop structure of HIV-$1_{V3L\#08}$ did not affect viral assembly and budding. Increased virus production from PM1/CCR5 cells was

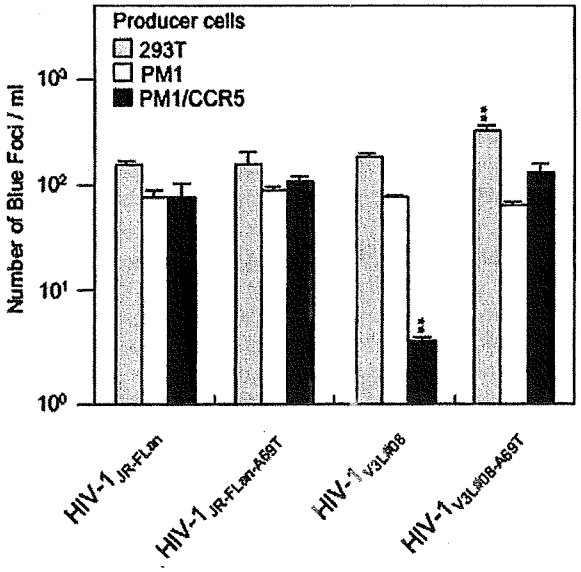

FIGURE 6. **Viral infectivity of HIV-$1_{JR-FLan}$, HIV-$1_{JR-FLan-A69T}$, HIV-$1_{V3L\#08}$, and HIV-$1_{V3L\#08-A69T}$ generated from 293T, PM1, or PM1/CCR5 cells.** Viral infectivity was determined with MAGIC5 cells (HeLa cells expressing CD4 and CCR5 and containing -galactosidase expression cassettes driven by the HIV-1 long terminal repeat). MAGIC5 cells were infected with each virus for 2 h. At 48 h post-infection, the cells were fixed and stained with 5-bromo-4-chloro-3-indolyl- -D-galactoside. The number of blue foci was counted in triplicate. The analysis was repeated three times; *error bars* represent S.D. of three replicates. *, p 0.01; **, p 0.001. Statistical significant differences were calculated by t test *versus* HIV-$1_{JR-FLan}$.

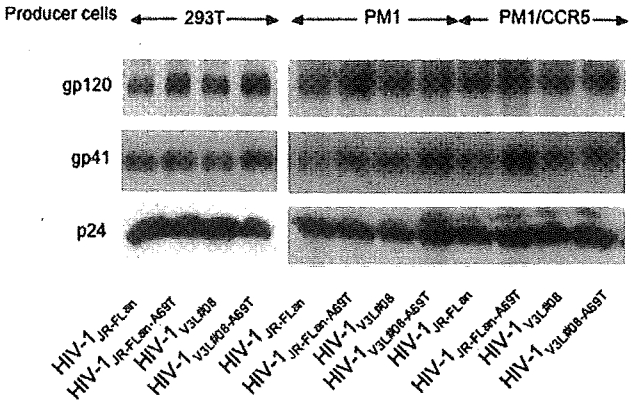

FIGURE 7. **Incorporation of gp120 and gp41 into virus.** HIV-$1_{JR-FLan}$, HIV-$1_{JR-FLan-A69T}$, HIV-$1_{V3L\#08}$, and HIV-$1_{V3L\#08-A69T}$ (100 ng of p24 Gag) produced from 293T, PM1, or PM1/CCR5 cells was resolved by 4–20% SDS-PAGE. Western blot analysis was performed using polyclonal antibody to gp120, gp41, and p24 Gag.

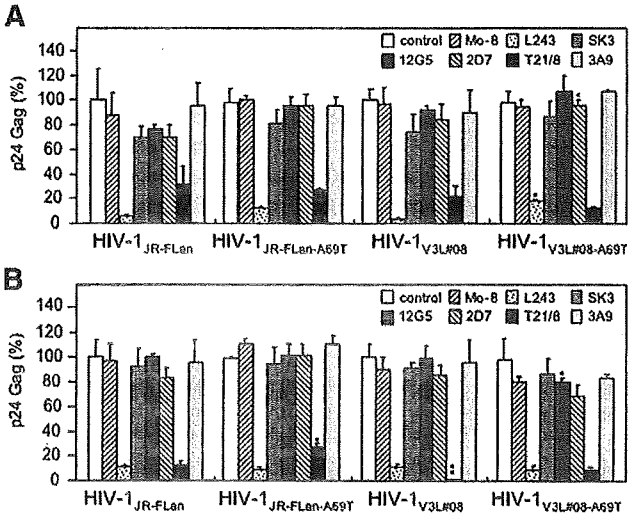

FIGURE 8. **Incorporation of CCR5 into virus.** Virus immunoprecipitation assay was performed using mAbs directed against hepatitis C virus (MO-8), HLA-DR (L243), CD4 (SK3), CXCR4 (12G5), or CCR5 (2D7, T21/8, 3A9). Cell-free virus (5 ng), produced from PM1 (*A*) or PM1/CCR5 (*B*) cells was incubated with 1 g of mAb for 8 h. Virus-antibody complex were precipitated by the addition of Pansorbin cells. After precipitation of the virus-antibody complex, p24 Gag in supernatants were determined by p24 Gag ELISA. The analysis was repeated three times; *error bars* represent S.D. of three replicates. *, p 0.01; **, p 0.001. Statistical significant differences were calculated by t test *versus* HIV-$1_{JR-FLan}$.

consistent with the higher entry efficiency, as shown in Fig. 4, although the increased levels were not equal. This excluded the possibility that replication suppression of HIV-$1_{V3L\#08}$ in PM1/CCR5 cells was due to decreased virus production.

HIV-$1_{V3L\#08}$ Infectivity Generated from PM1/CCR5 Cells—To further investigate replication suppression of HIV-$1_{V3L\#08}$ in PM1/CCR5 cells, infectivity of viruses generated from 293T, PM1, and PM1/CCR5 cells was determined using MAGIC5 cells containing a -galactosidase gene driven by the HIV long terminal repeat (37) (Fig. 6). Infectivity from 293T cells, used for experimental preparation of viruses, was similar among the four viruses. However, infectivity of HIV-$1_{V3L\#08}$ generated from PM1/CCR5 cells showed a 20-fold decrease compared with HIV-$1_{JR-FLan}$, whereas infectivity of viruses, including HIV-$1_{V3L\#08}$ from PM1 cells, revealed similar infectivity. Note that HIV-$1_{V3L\#08-A69T}$, with an additional substitution of Ala^{69} to Thr plus the eight amino acid substitutions of HIV-$1_{V3L\#08}$, reacquired a potent infection ability from PM1/CCR5 cells. The decrease infectivity in progeny HIV-$1_{V3L\#08}$ from PM1/CCR5 cells could result in impaired replication of HIV-$1_{V3L\#08}$ in PM1/CCR5 cells, as shown in Fig. 3*B*.

CCR5 Incorporation into HIV-$1_{V3L\#08}$ Virions—To elucidate the significance of CCR5 levels on decreased infectivity in HIV-$1_{V3L\#08}$, we examined whether high expression of CCR5 inhibits its incorporation of Env proteins gp120 and gp41 into virus particles. Amounts of gp120 and gp41 on the virus envelopes were compared (Fig. 7). There was no decrease in gp120 and gp41 in HIV-$1_{V3L\#08}$ generated from PM1/CCR5 cells, indicating that high levels of CCR5 has no effect on the incorporation efficiency of gp120 and gp41 into the virions. A slight increase in gp120 and gp41 incorporation into virions was observed in HIV-$1_{JR-FLan-A69T}$ and HIV-$1_{V3L\#08-A69T}$ compared to HIV-$1_{JR-FLan}$ and HIV-$1_{V3L\#08}$ generated from 293T, PM1, and PM1/CCR5 cells. The increased gp120 and gp41 incorporation into virions by the addition of A69T may be in compensation for the loss of infectivity in HIV-$1_{V3L\#08}$ from PM1/CCR5 cells.

Another putative mechanism could be that CCR5 is incorporated into virus particles and specifically impaired the intrinsic function of HIV-$1_{V3L\#08}$ gp120. To examine this possibility, the virions were precipitated using anti-CCR5 mAbs (Fig. 8, *A* and *B*). It has been reported that HLA-DR is incorporated into the viral envelope from the infected cell membrane (42, 43). We confirmed that an anti-HLA-DR mAb L243 could precipitate

TABLE 2
Replication of HIV-1 containing one amino acid substitution in V3 loop in PM1 and PM1/CCR5 cells

Viral clone	V3 loop sequence	p24 Gag (ng/ml)[a] PM1	PM1/CCR5	Ratio[b]
HIV-$1_{JR-Flan}$	CTRPNNNTRKSIHIGPGRAFYTTGEIIGDIRQAHC	140	270	1.9
HIV-$1_{V3\#08}$	.....VTM.....L.A..DV..N.....	83	8.0	0.1
HIV-1_{I307V}	.....V.....	100	11	0.1
HIV-1_{H308T}	.....T.....	79	100	1.3
HIV-1_{I309M}	.....M.....	63	9.0	0.1
HIV-1_{F315L}	.....L.....	59	14	0.2
HIV-1_{T317A}	.....A.....	<1.0	<1.0	–
HIV-1_{E320D}	.....D.....	110	72	0.7
HIV-1_{I321V}	.....V.....	91	110	1.2
HIV-1_{D324N}	.....N.....	75	68	0.9

[a] PM1 or PM1/CCR5 cells (4 10^4) were infected with each virus (8 ng of p24 Gag). On day 6 the extent of viral replication was measured by p24 Gag ELISA. Results represent the average of three independent experiments.
[b] Ratio, the concentration of p24 Gag in the supernatant of PM1/CCR5 cells was divided by that of PM1 cells.

virions generated from PM1 or PM1/CCR5 cells, whereas anti-E2 protein mAb of hepatitis C virus Mo-8, anti-CD4 mAb SK3, or anti-CXCR4 12G5 could not. mAb 2D7 (44), which could recognize the second extracellular loop of CCR5 on the surface of PM1 or PM1/CCR5 cells via flow cytometry (Fig. 2), failed to precipitate viral particles (Fig. 8, *A* and *B*). Similarly, 3A9 (45), an anti-CCR5 mAb recognizing the N terminus via flow cytometry (data not shown), could not precipitate viruses either. Surprisingly, another anti-CCR5 mAb (T21/8), also recognizing the N terminus, partially precipitated viruses generated from PM1 (Fig. 8*A*) and PM1/CCR5 cells (Fig. 8*B*) but not from 293T cells (data not shown). Note that HIV-$1_{V3L\#08}$ generated from PM1/CCR5 cells was almost completely precipitated (98%) by mAb T21/8 (Fig. 8*B*), whereas HIV-$1_{V3L\#08}$ generated from PM1 cells and the other three viruses from both cell types were partially precipitated (69–88%) by mAb T21/8 (Fig. 8*A*). The results indicate that sufficient levels of CCR5 were incorporated into HIV-$1_{V3L\#08}$ particles to be precipitated by T21/8. The larger amount of incorporated CCR5 reduced viral infectivity in HIV-$1_{V3L\#08}$, although the recruitment of CCR5 into virions and the molecular mechanism of decreased infectivity in HIV-$1_{V3L\#08}$ are unclear. For comparison of the amount of CCR5 at the surface of the virions, we purified virions by precipitation using anti-gp120 antibody 2G12 from exosomes contaminated in the virion by Western blot analysis. However, we could not detect CCR5 possibly because of low affinity of anti-CCR5 antibodies (data not shown).

Amino Acid Substitutions in the V3 Loop Responsible for $R5^L$ Phenotype—In 45 viral clones, three viruses revealed an $R5^L$ phenotype (Table 1). The amino acid substitutions Ile^{307} to Val and Ile^{309} to Met were common to all three viruses, suggesting that these two substitutions could be responsible for the $R5^L$ phenotype. To assess the contribution of the eight substitutions in the HIV-$1_{V3L\#08}$ V3 loop to the $R5^L$ phenotype, eight V3 loop mutant viruses containing one substitution each were prepared, and their replication phenotypes were determined (Table 2). Replication of HIV-1_{I307V} and HIV-1_{I309M} was suppressed in PM1/CCR5 cells, whereas these viruses could replicate in PM1 cells (60 ng/ml p24 Gag), consistent with the common substitutions obtained in three $R5^L$ viruses described above (Table 1).

To ascertain the importance of these substitutions, V3 mutant viruses containing random combinations of between two and six of the eight substitutions from HIV-$1_{V3L\#08}$ were prepared. Most of the recombinant viruses preferentially replicate in PM1 cells (ratio 0.5) (Table 3). Four of 12 viruses revealed a $R5^L$ phenotype (ratio 0.1) and contained I307V and/or I309M. Viruses containing I307V always showed a low p24 Gag ratio (ratio 0.3), whereas ratios in I309M-containing viruses were not as low (Fig. 9), *e.g.* 1.4 for HIV-$1_{V3L\#130}$ (Table 3). In addition, F315L frequently conferred a low p24 Gag ratio combined with other substitutions, although F315L alone could not confer $R5^L$ phenotype. The results show that the $R5^L$ phenotype cannot be conferred by just one or two substitutions; a combination of several substitutions, including key substitutions, is essential. The key amino acid residues at 307 and 309 were directly at the N-terminal of the GPGR sequence in the V3 loop crown, suggesting that the amino acid substitutions adjoining the V3 crown may be important in regulating replication kinetics in cells expressing high levels of CCR5.

DISCUSSION

We investigated the replication ability of 45 viral clones from the R5 HIV-1 V3 loop library and found that the library contained different replication phenotypes with respect to the expression level of CCR5 (Table 1). The report focused on one of the viruses, HIV-$1_{V3L\#08}$, that was suppressed 33-fold in PM1/CCR5 cells expressing high levels of CCR5 compared with parental PM1 cells (Fig. 3*B*). This suppression of viral growth was not associated with early events in the lifecycle but with a decrease in viral infectivity in nascent progeny virus from cells expressing high levels of CCR5. MAGIC5 (37) and NP2/CD4/hiCCR5 cells expressed CD4 at levels similar to and CCR5 at levels compatible to or higher than that of PM1/CCR5 cells;

TABLE 3
Replication of HIV-1 containing a random combination of the eight amino acid substitutions from HIV-$1_{V3L\#08}$ V3 loop in PM1 and PM1/CCR5 cells

Viral clone	V3 loop sequence	p24 Gag (ng/ml)[a] PM1	PM1/CCR5	Ratio[b]
HIV-$1_{JR\text{-}FLan}$	CTRPNNNTRKSIHIGPGRAFYTTGEIIGDIRQAHC	140	270	1.9
HIV-$1_{V3L\#08}$	.....VTM.....L.A..DV..N.....	83	8.0	< 0.1
HIV-$1_{V3L\#102}$	.....T.....L.....N.....	200	72	0.4
HIV-$1_{V3L\#103}$	.....TM.....DV.....	150	<1.0	< 0.1
HIV-$1_{V3L\#104}$	.....VT.....A..DV..N.....	210	84	0.4
HIV-$1_{V3L\#117}$	.....VT.....L.A...V.....	110	<1.0	< 0.1
HIV-$1_{V3L\#121}$	.....VT.....L.....V.....	120	<1.0	< 0.1
HIV-$1_{V3L\#124}$	.....TM.....A..DV.....	150	40	0.3
HIV-$1_{V3L\#125}$	.....T.....A.....	14	170	11
HIV-$1_{V3L\#127}$	.....VTM.....L.A.....N.....	200	<1.0	< 0.1
HIV-$1_{V3L\#128}$	.....VT.....L.A..D...N.....	160	30	0.2
HIV-$1_{V3L\#130}$	.....M.....A..D...N.....	130	180	1.4
HIV-$1_{V3L\#132}$	.....TM.....V.....	160	70	0.4
HIV-$1_{V3L\#133}$	.....VT.....A...V..N.....	120	20	0.2

[a] PM1 or PM1/CCR5 cells (4 10^4) were infected with each virus (8 ng of p24 Gag). On day 6 the extent of viral replication was measured by p24 Gag antigen ELISA. Results represent the average of three independent experiments.
[b] Ratio, the concentration of p24 Gag in the supernatant of PM1/CCR5 cells was divided by that of PM1 cells.

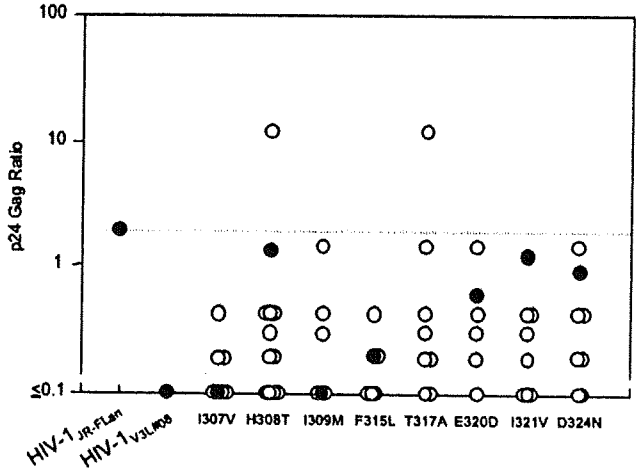

FIGURE 9. **Effect of each amino acid substitution on preferential replication of V3 mutant viruses.** Ratios of p24 Gag in seven mutant viruses in Table 2 and 12 mutant viruses in Table 3 were plotted. *Closed circle*, mutant virus containing one substitution in the V3 loop (Table 2). *Open circle*, virus containing a random combination of multiple substitutions in the HIV-$1_{V3L\#08}$ V3 loop (Table 3).

however, HIV-$1_{V3L\#08}$ showed no CCR5-dependent replication suppression compared with MAGI/CCR5, NP2/CD4/lowCCR5 expressing a similar level of CD4, and a lower level of CCR5 (data not shown). The results suggest that distribution or localization of CCR5 on the surface in PM1 cell line may be distinct from these adherent cells.

Depending on the surface of the host cell, HIV-1 incorporates cell-derived molecules into its envelope (46, 47). HLA-DR, $_2$-microglobulin, ICAM-1 (intercellular adhesion molecule 1), and other cellular surface proteins were incorporated into a budding virion (48, 49), whereas CD4, CXCR4, and CCR5 were not detectable (50). Using the anti-CCR5 mAb, T21/8, we found CCR5 incorporated into a budding virion (Fig. 8). In contrast, two anti-CCR5 mAbs, 2D7 and 3A9, failed to capture virions from PM1 and PM1/CCR5 cells despite the fact that 2D7 (Fig. 2) and 3A9 (data not shown) could recognize CCR5 at the cell surface, indicating that the epitopes of 2D7 and 3A9 were lost by conformation change or concealed from the antibodies by interaction with other molecule(s) on a virus particle. The epitope of 2D7 is mapped to the second extracellular loop including Lys^{171}-Glu^{172} by alanine mutagenesis scan (44). The tertiary structure of CCR5 including Ser^7 and $^9IYD^{11}$ in the N terminus and His^{88} and Trp^{94} in the first extracellular loop are estimated to contribute to the binding of 3A9 by phage displayed peptide libraries (45), whereas T21/8 epitope has not been mapped but should be located in the N terminus of 22 amino acid residues from Met^1 to Lys^{22}; T21/8 was raised against a peptide corresponding to residues 1–22 of CCR5 according to the manufacturer. For viral entry, binding of coreceptors to HIV-1 gp120 is mediated by the V3 loop and the coreceptor-binding site located in the bridging sheet of gp120 (12, 14–16). The N terminus and the first and second extracellular loops of CCR5 are thought to interact with gp120 (51, 52). Loss of 2D7 and 3A9 binding with CCR5 at the viral envelope indicate that conformation of CCR5 at the viral envelope is distinct from that of CCR5 at the host cell surface.

The following scenario could explain the decreased infectivity in HIV-$1_{V3L\#08}$ from PM1/CCR5 cells. In HIV-$1_{V3L\#08\text{-}A69T}$, HIV-$1_{JR\text{-}FLan}$, and HIV-$1_{JR\text{-}FLan\text{-}A69T}$ generated from PM1 and PM1/CCR5 cells, cellular CCR5 is incorporated into the virion envelope but does not impair viral infectivity due to the low level of CCR5. A similar amount of CCR5 incorporated into HIV-$1_{V3L\#08}$ from PM1 cells is not sufficient to impair viral

infectivity either. Larger amounts of CCR5 are recruited by HIV-$1_{V3L\#08}$ from the PM1/CCR5 cell surface into the virions, and the CCR5 levels are above the threshold needed for suppression of viral replication. HIV-$1_{V3L\#08}$ from PM1/CCR5 cells was almost completely precipitated by T21/8, indicating that most of the virus particles contained sufficient levels of CCR5 for capture (Fig. 8*B*), although immunoprecipitation efficiency of virions does not proportionally reflect the amount of CCR5. Otherwise incorporated CCR5 may specifically impair gp120 and gp41 function by an unknown mechanism through the HIV-$1_{V3L\#08}$ V3 loop or via recruitment of nonfunctional gp120-CCR5 complexes at the virion surface. Loss of infectivity seems to be V3-dependent (Tables 2 and 3), and amino acid substitutions near the V3 tip may play a pivotal role on the complex-formation on virions. However, the role of the point mutation of C1 in the revertant virus (HIV-$1_{V3L\#08\text{-}A69T}$) on V3 conformation or amount of gp120 and gp41 on virions (Fig. 7) is still murky. Another possibility is that CCR5 interacts with HIV-$1_{V3L\#08}$ gp120 between virus-virus envelopes in the *trans* position without CD4; the interaction between viral particles through CCR5 and gp120 leads to decrease of viral infectivity, although this is unlikely. To further elucidate incorporation of CCR5 into a virus particle and decrease of viral infectivity, the molecular behavior of CCR5 and HIV-$1_{V3L\#08}$ gp120 in PM1/CCR5 cells needs to be studied.

There are several reports for donor-dependent variations in CCR5 expression even among donors who do not possess the CCR5 32 allele, with a 20-fold variation in CCR5 expression on peripheral blood mononuclear cells from human donors being reported (53, 54). CCR5 expression levels in the target cells might be a source of alternative selective pressure on the development of the HIV-1 envelope *in vivo*, although the range of expression from PM1 to PM1/CCR5 cells is supposed to be higher than in CCR5-expressing cells *in vivo*.

Thus, high CCR5 expression does not always benefit replication in all R5 HIV-1. The same V3 loop sequence for the $R5^L$ phenotype, including HIV-$1_{V3L\#08}$, HIV-$1_{V3L\#23}$, and HIV-$1_{V3L\#25}$, could not be found in the data base of HIV-1 clinical isolates, suggesting that HIV-1 has evolved to overcome problems in viral replication caused by the high expression levels of CCR5 in target cells *in vivo*. The results demonstrate the significant implications of an alternative influence of CCR5 on R5 HIV-1 replication.

Acknowledgments—We thank Akiko Honda and Kazuhisa Yoshimura for technical advice on real-time PCR and Tetsuya Kimura for scientific discussion.

REFERENCES

1. Berger, E. A., Doms, R. W., Fenyo, E. M., Korber, B. T., Littman, D. R., Moore, J. P., Sattentau, Q. J., Schuitemaker, H., Sodroski, J., and Weiss, R. A. (1998) *Nature* **391,** 240
2. Doms, R. W., and Peiper, S. C. (1997) *Virology* **235,** 179–190
3. Moore, J. P., Trkola, A., and Dragic, T. (1997) *Curr. Opin. Immunol.* **9,** 551–562
4. Lin, Y. L., Mettling, C., Portales, P., Reynes, J., Clot, J., and Corbeau, P. (2002) *Proc. Natl. Acad. Sci. U. S. A.* **99,** 15590–15595
5. Peters, P. J., Bhattacharya, J., Hibbitts, S., Dittmar, M. T., Simmons, G., Bell, J., Simmonds, P., and Clapham, P. R. (2004) *J. Virol.* **78,** 6915–6926
6. Platt, E. J., Wehrly, K., Kuhmann, S. E., Chesebro, B., and Kabat, D. (1998) *J. Virol.* **72,** 2855–2864
7. Reynes, J., Baillat, V., Portales, P., Clot, J., and Corbeau, P. (2003) *J. Acquired Immune Defic. Syndr.* **34,** 114–116
8. Walter, B. L., Wehrly, K., Swanstrom, R., Platt, E., Kabat, D., and Chesebro, B. (2005) *J. Virol.* **79,** 4828–4837
9. Kwong, P. D., Wyatt, R., Robinson, J., Sweet, R. W., Sodroski, J., and Hendrickson, W. A. (1998) *Nature* **393,** 648–659
10. Trkola, A., Dragic, T., Arthos, J., Binley, J. M., Olson, W. C., Allaway, G. P., Cheng-Mayer, C., Robinson, J., Maddon, P. J., and Moore, J. P. (1996) *Nature* **384,** 184–187
11. Wyatt, R., Kwong, P. D., Desjardins, E., Sweet, R. W., Robinson, J., Hendrickson, W. A., and Sodroski, J. G. (1998) *Nature* **393,** 705–711
12. Reeves, J. D., Gallo, S. A., Ahmad, N., Miamidian, J. L., Harvey, P. E., Sharron, M., Pohlmann, S., Sfakianos, J. N., Derdeyn, C. A., Blumenthal, R., Hunter, E., and Doms, R. W. (2002) *Proc. Natl. Acad. Sci. U. S. A.* **99,** 16249–16254
13. Reeves, J. D., Miamidian, J. L., Biscone, M. J., Lee, F. H., Ahmad, N., Pierson, T. C., and Doms, R. W. (2004) *J. Virol.* **78,** 5476–5485
14. Rizzuto, C. D., Wyatt, R., Hernandez-Ramos, N., Sun, Y., Kwong, P. D., Hendrickson, W. A., and Sodroski, J. (1998) *Science* **280,** 1949–1953
15. Rizzuto, C., and Sodroski, J. (2000) *AIDS Res. Hum. Retroviruses* **16,** 741–749
16. Suphaphiphat, P., Thitithanyanont, A., Paca-Uccaralertkun, S., Essex, M., and Lee, T. H. (2003) *J. Virol.* **77,** 3832–3837
17. Wu, L., Gerard, N. P., Wyatt, R., Choe, H., Parolin, C., Ruffing, N., Borsetti, A., Cardoso, A. A., Desjardin, E., Newman, W., Gerard, C., and Sodroski, J. (1996) *Nature* **384,** 179–183
18. Wyatt, R., and Sodroski, J. (1998) *Science* **280,** 1884–1888
19. Zhang, W., Canziani, G., Plugariu, C., Wyatt, R., Sodroski, J., Sweet, R., Kwong, P., Hendrickson, W., and Chaiken, I. (1999) *Biochemistry* **38,** 9405–9416
20. Delwart, E. L., and Panganiban, A. T. (1989) *J. Virol.* **63,** 273–280
21. Steck, F. T., and Rubin, H. (1966) *Virology* **29,** 628–641
22. Aiken, C., Konner, J., Landau, N. R., Lenburg, M. E., and Trono, D. (1994) *Cell* **76,** 853–864
23. Bresnahan, P. A., Yonemoto, W., Ferrell, S., Williams-Herman, D., Geleziunas, R., and Greene, W. C. (1998) *Curr. Biol.* **8,** 1235–1238
24. Craig, H. M., Pandori, M. W., and Guatelli, J. C. (1998) *Proc. Natl. Acad. Sci. U. S. A.* **95,** 11229–11234
25. Greenberg, M., DeTulleo, L., Rapoport, I., Skowronski, J., and Kirchhausen, T. (1998) *Curr. Biol.* **8,** 1239–1242
26. Mangasarian, A., Foti, M., Aiken, C., Chin, D., Carpentier, J. L., and Trono, D. (1997) *Immunity* **6,** 67–77
27. Piguet, V., Chen, Y. L., Mangasarian, A., Foti, M., Carpentier, J. L., and Trono, D. (1998) *EMBO J.* **17,** 2472–2481
28. Geleziunas, R., Bour, S., and Wainberg, M. A. (1994) *FASEB J.* **8,** 593–600
29. Willey, R. L., Maldarelli, F., Martin, M. A., and Strebel, K. (1992) *J. Virol.* **66,** 7193–7200
30. Palese, P., Tobita, K., Ueda, M., and Compans, R. W. (1974) *Virology* **61,** 397–410
31. Lama, J., Mangasarian, A., and Trono, D. (1999) *Curr. Biol.* **9,** 622–631
32. Levesque, K., Zhao, Y. S., and Cohen, E. A. (2003) *J. Biol. Chem.* **278,** 28346–28353
33. Michel, N., Allespach, I., Venzke, S., Fackler, O. T., and Keppler, O. T. (2005) *Curr. Biol.* **15,** 714–723
34. Yusa, K., Maeda, Y., Fujioka, A., Monde, K., and Harada, S. (2005) *J. Biol. Chem.* **280,** 30083–30090
35. Lusso, P., Cocchi, F., Balotta, C., Markham, P. D., Louie, A., Farci, P., Pal, R., Gallo, R. C., and Reitz, M. S., Jr. (1995) *J. Virol.* **69,** 3712–3720
36. Maeda, Y., Foda, M., Matsushita, S., and Harada, S. (2000) *J. Virol.* **74,** 1787–1793
37. Hachiya, A., Aizawa-Matsuoka, S., Tanaka, M., Takahashi, Y., Ida, S., Gatanaga, H., Hirabayashi, Y., Kojima, A., Tatsumi, M., and Oka, S. (2001) *Antimicrob. Agents Chemother.* **45,** 495–501
38. Mariani, R., Rutter, G., Harris, M. E., Hope, T. J., Krausslich, H. G., and

Landau, N. R. (2000) *J. Virol.* **74,** 3859–3870
39. Kimpton, J., and Emerman, M. (1992) *J. Virol.* **66,** 2232–2239
40. Esser, M. T., Graham, D. R., Coren, L. V., Trubey, C. M., Bess, J. W., Jr., Arthur, L. O., Ott, D. E., and Lifson, J. D. (2001) *J. Virol.* **75,** 6173–6182
41. Inudoh, M., Kato, N., and Tanaka, Y. (1998) *Microbiol. Immunol.* **42,** 875–877
42. Cantin, R., Fortin, J. F., Lamontagne, G., and Tremblay, M. (1997) *Blood* **90,** 1091–1100
43. Cantin, R., Fortin, J. F., Lamontagne, G., and Tremblay, M. (1997) *J. Virol.* **71,** 1922–1930
44. Lee, B., Sharron, M., Blanpain, C., Doranz, B. J., Vakili, J., Setoh, P., Berg, E., Liu, G., Guy, H. R., Durell, S. R., Parmentier, M., Chang, C. N., Price, K., Tsang, M., and Doms, R. W. (1999) *J. Biol. Chem.* **274,** 9617–9626
45. O'Connor, K. H., Konigs, C., Rowley, M. J., Irving, J. A., Wijeyewickrema, L. C., Pustowka, A., Dietrich, U., and Mackay, I. R. (2005) *J. Immunol. Methods* **299,** 21–35
46. Ott, D. E. (2002) *Rev. Med. Virol.* **12,** 359–374
47. Tremblay, M. J., Fortin, J. F., and Cantin, R. (1998) *Immunol. Today* **19,** 346–351
48. Hoxie, J. A., Fitzharris, T. P., Youngbar, P. R., Matthews, D. M., Rackowski, J. L., and Radka, S. F. (1987) *Hum. Immunol.* **18,** 39–52
49. Ott, D. E. (1997) *Rev. Med. Virol.* **7,** 167–180
50. Lallos, L. B., Laal, S., Hoxie, J. A., Zolla-Pazner, S., and Bandres, J. C. (1999) *AIDS Res. Hum. Retroviruses* **15,** 895–897
51. Dragic, T., Trkola, A., Lin, S. W., Nagashima, K. A., Kajumo, F., Zhao, L., Olson, W. C., Wu, L., Mackay, C. R., Allaway, G. P., Sakmar, T. P., Moore, J. P., and Maddon, P. J. (1998) *J. Virol.* **72,** 279–285
52. Farzan, M., Choe, H., Vaca, L., Martin, K., Sun, Y., Desjardins, E., Ruffing, N., Wu, L., Wyatt, R., Gerard, N., Gerard, C., and Sodroski, J. (1998) *J. Virol.* **72,** 1160–1164
53. Moore, J. P. (1997) *Science* **276,** 51–52
54. Wu, L., Paxton, W. A., Kassam, N., Ruffing, N., Rottman, J. B., Sullivan, N., Choe, H., Sodroski, J., Newman, W., Koup, R. A., and Mackay, C. R. (1997) *J. Exp. Med.* **185,** 1681–1691

Journal of General Virology (2007), **88**, 3139–3144 DOI 10.1099/vir.0.83202-0

Short Communication

Inhibitory role of CXCR4 glycan in CD4-independent X4-tropic human immunodeficiency virus type 1 infection and its abrogation in CD4-dependent infection

Yoshinao Kubo,[1] Masaru Yokoyama,[1,2] Hiroaki Yoshii,[1] Chiho Mitani,[1] Chika Tominaga,[1] Yuetsu Tanaka,[3] Hironori Sato[1,2] and Naoki Yamamoto[1,4,5]

Correspondence
Yoshinao Kubo
yoshinao@net.nagasaki-u.ac.jp

[1]Department of AIDS Research, Institute of Tropical Medicine, Nagasaki University, Nagasaki, Japan

[2]Laboratory of Viral Genomics, Center for Pathogen Genomics, National Institute of Infectious Diseases, Tokyo, Japan

[3]Department of Immunology, Graduate School and Faculty of Medicine, University of the Ryukyus, Okinawa, Japan

[4]AIDS Research Center, National Institute of Infectious Diseases, Tokyo, Japan

[5]Department of Molecular Virology, Tokyo Medical and Dental University, Tokyo, Japan

CXCR4 functions as an infection receptor of X4 human immunodeficiency virus type 1 (HIV-1). CXCR4 is glycosylated at the N-terminal extracellular region, which is important for viral envelope (Env) protein binding. We compared the effects of CXCR4 glycan on the CD4-dependent and -independent infections in human cells by X4 viruses. We found that transduction mediated by Env proteins of CD4-independent HIV-1 strains increased up to 5.5-fold in cells expressing unglycosylated CXCR4, suggesting that the CXCR4 glycan inhibits CD4-independent X4 virus infection. Co-expression of CD4 on the target cell surface or pre-incubation of virus particles with soluble CD4 abrogates the glycan-mediated inhibition of X4 virus infection, suggesting that interaction of Env protein with CD4 counteracts the inhibition. These findings indicate that it will be advantageous for X4 HIV-1 to remain CD4-dependent. A structural model that explains the glycan-mediated inhibition is discussed.

Received 1 June 2007
Accepted 18 July 2007

Infection by the X4-tropic human immunodeficiency virus type 1 (HIV-1) requires interaction of two cellular surface proteins, CD4 and CXCR4 (Berger *et al.*, 1998; Dimitrov, 1997). CXCR4 is a multi-membrane-spanning protein that possesses an N-glycosylation site in the N-terminal extracellular region (Chabot *et al.*, 2000). Since the glycosylation site locates near the amino acid residues important for HIV-1 entry (Brelot *et al.*, 2000; Chabot & Broder, 2000; Chabot *et al.*, 1999; Picard *et al.*, 1997), the glycan may inhibit X4 virus infection. Consistently, previous studies using mink or canine cells have indicated that the glycan inhibits infections of HIV-1 and HIV-2 X4 viruses (Potempa *et al.*, 1997; Wang *et al.*, 2004). However, it is not known whether the glycan has the same effect in human cells, in which glycan modification or other cellular cofactors necessary for infection might be different from those in non-human cells. Furthermore, studies using human cells failed to observe such inhibitory effects (Brelot *et al.*, 2000; Chabot *et al.*, 2000; Picard *et al.*, 1997; Thordsen *et al.*, 2002). Thus, despite extensive studies, the role of the CXCR4 glycan in X4 virus infection remained to be determined.

As is the case for HIV-1, most simple retroviruses use N-glycosylated multi-membrane-spanning proteins as their receptors (Overbaugh *et al.*, 2001; Sommerfelt, 1999). In contrast to the HIV-1 studies, however, all the studies reproducibly indicated that the N-glycan on the receptors can efficiently suppress simple retrovirus infection (Kubo *et al.*, 2002; Marin *et al.*, 2003; Tailor *et al.*, 2000; Wilson & Eiden, 1991). Entry mechanisms of the simple retroviruses and HIV-1 are similar in that they use multi-membrane-spanning proteins, whereas they differ in that the simple retroviruses need only a single type of receptor. Therefore, we hypothesized that the initial binding of gp120 to CD4 might counteract the glycan-mediated block of X4 virus infection.

Supplementary material is available with the online version of this paper.

To examine this hypothesis, we established human NP2 and U87 cell lines (Soda *et al.*, 1999) that express C-terminally HA-tagged wild-type (wt) CXCR4 or N11A mediated by a murine leukaemia virus vector as reported previously (Kubo *et al.*, 2003). N11A is a CXCR4 mutant lacking the N-glycosylation site by substitution of the asparagine residue by an alanine (Fig. 1a). Western immunoblot analysis using the anti-HA monoclonal antibody showed that N11A migrated faster than wt CXCR4, consistent with the loss of the N-glycan by mutation (Supplementary Figure S1, available with the online version of this paper).

We examined if the lack of the glycan on CXCR4 could affect transduction titres of an HIV-1 vector (Naldini *et al.*, 1996) having CD4-independent mNDK (Dumonceaux *et al.*, 1998) or 8X (Hoffman *et al.*, 1999) HIV-1 gp120. The HIV-1 vector contains the *lacZ* gene as a marker (Chang *et al.*, 1999; Iwakuma *et al.*, 1999), and transduction titre was estimated by counting blue cells after X-Gal staining of the inoculated cells as reported previously (Kubo *et al.*, 2004). Infection of the NP2 and U87 cells expressing N11A resulted in a moderate but statistically significant increase in the mNDK transduction titres; titres in N11A-expressing cells were about 1.5 and 2.5-fold higher than those in wt-expressing cells (Fig. 1b). Levels of enhancement were greater with 8X vector; titres in N11A-expressing cells were about 2.0 and 5.5-fold higher than those in wt-expressing cells. In contrast, the lack of glycan did not cause significant changes in titres of the VSV-G-pseudotyped vector (Chang *et al.*, 1999).

We analysed levels of cell-surface expression of wt and N11A CXCR4 in NP2 and U87 cells by FACS with an anti-CXCR4 antibody (A80) that recognizes the third extracellular loop of CXCR4 (Tanaka *et al.*, 2001). Fluorescence intensities of N11A-expressing NP2 and U87 cells were about 2 to 10-fold lower than those of wt-expressing cells (Fig. 1c). If wt and N11A were expressed at the same level, N11A could be 15 to 25 times more susceptible to CD4-independent infection than wt in NP2 cells. Similarly, N11A could be 4 to 11 times more susceptible than wt in U87 cells. This indicates that the CXCR4 glycan significantly inhibits CD4-independent infection. However, treatment of wt CXCR4-expressing cells with tunicamycin, an N-glycosylation inhibitor, had severe cytotoxicity, especially in U87 cells, and did not increase 8X vector transduction titre.

We examined whether the CXCR4 glycan could influence X4 virus infection upon CD4-mediated infection. For this purpose, we established NP2 and U87 cell lines that express both CD4 and CXCR4. As was seen with the CD4-negative cell lines, the size of N11A was smaller than that of wt (Supplementary Figure S2, available with the online version of this paper). Similarly, fluorescence intensities of N11A-expressing NP2 and U87 cells detected by FACS analysis were about 2 and 10-fold lower than those of wt-expressing cells in CD4-positive cells, respectively (Fig. 2a and b).

We next measured the effect of CD4 expression on transduction efficiency of various Env-pseudotyped vectors. Transduction titres of the mNDK and 8X vectors in NP2 cells co-expressing CXCR4 and CD4 were about 100-fold higher than in cells expressing CXCR4 alone (Supplementary Figure S3, available with the online version of this paper), suggesting that constitutive exposure of the coreceptor-binding site in these CD4-independent gp120 is partial and that CD4-induced conformational changes result in the full exposure.

We examined whether the CXCR4 glycan could influence X4 virus infection upon CD4-mediated infection. The

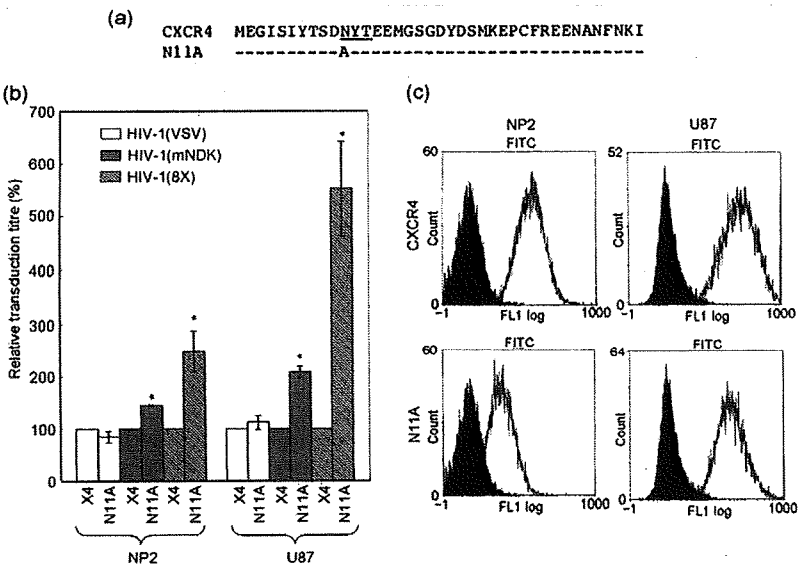

Fig. 1. Role of CXCR4 glycan in CD4-independent infection of X4 viruses. (a) Amino acid sequences of the N-terminal extracellular regions of wt CXCR4 and the N11A mutant. Hyphens indicate residues identical to wt CXCR4. The glycosylation site is underlined. The Asn residue was changed to Ala in the N11A mutant. (b) Relative transduction titres of the vectors in human cell lines expressing wt and N11A CXCR4. Relative titres to the titre in cells expressing wt CXCR4 (X4) are indicated. This experiment was repeated three times. Asterisks indicate statistical significance determined by Student's *t*-test, $P<0.05$. (c) Cell-surface expression was analysed with a flow cytometer and the anti-CXCR4 antibody (A80). The black area indicates control cells stained with the A80 antibody. The white area indicates wt CXCR4- and N11A mutant-expressing cells stained with the A80 antibody.

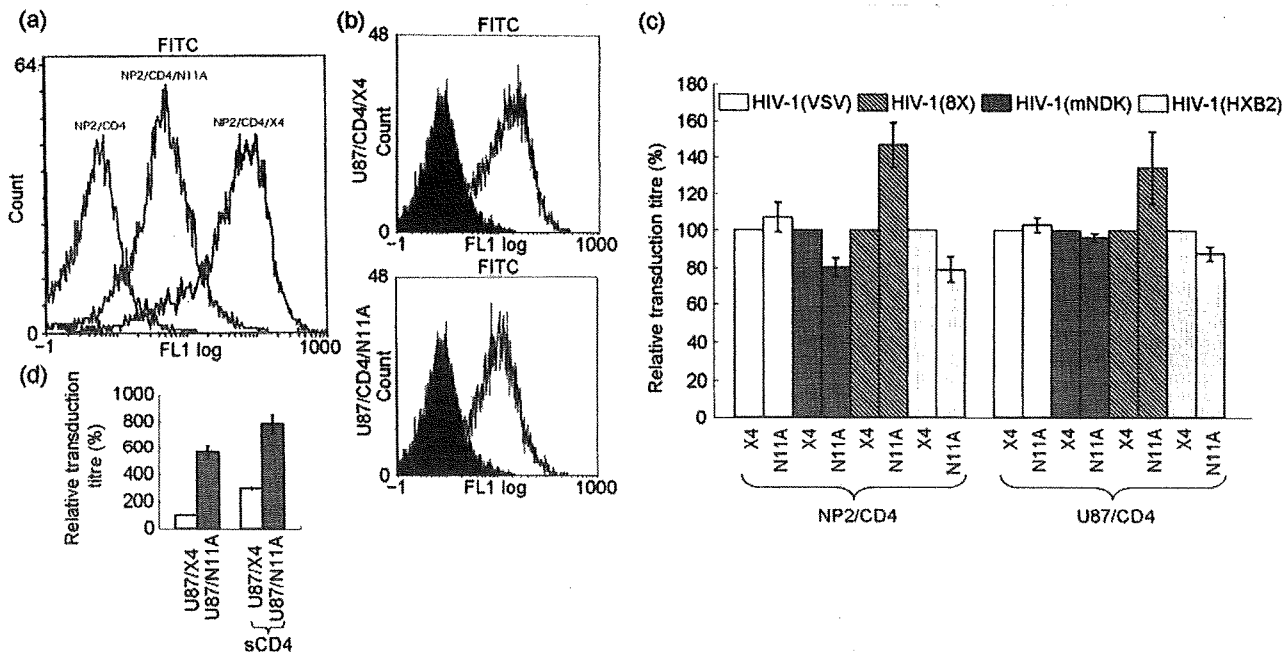

Fig. 2. CD4 counteracts CXCR4 glycan-mediated inhibition of X4 virus infection. (a, b) Cell-surface expression of wt CXCR4 and N11A mutant in NP2/CD4 (a) or U87/CD4 (b) cells was analysed with a flow cytometer and the anti-CXCR4 antibody A80. Black area indicates the control cells stained with A80. White area indicates wt CXCR4- and N11A mutant-expressing cells stained with A80. (c) Relative transduction titres of the vectors in human cells co-expressing CD4 and CXCR4. Relative titres to the titre in cells expressing CD4 and wt CXCR4 (X4) are indicated. Asterisks indicate statistical significance determined by Student's *t*-test, $P<0.05$. (d) Relative transduction titres of the 8X vector in the absence or presence of sCD4 (20 μg ml^{-1}). Relative titres to the titre in U87/X4 cells in the absence of sCD4 are indicated. These experiments were repeated three times.

vector solutions were diluted to obtain transduction titres similar to those of CD4-independent vectors in CD4-negative cells (about 5×10^2 infected cells per ml). Fig. 2(c) shows the relative transduction titres of the various Env-pseudotyped vectors in NP2 and U87 cells co-expressing CD4 and CXCR4. In contrast to the results with cells expressing N11A alone (Fig. 1), we could not detect a statistically significant increase in transduction titre of the vectors carrying the mNDK and the CD4-dependent HXB2 Env proteins in N11A-expressing cells. Similarly, removal of the CXCR4 glycan induced only a moderate increase in transduction titres of the 8X vector. These results showed that the mNDK, 8X and HXB2 viruses infected cells expressing wt CXCR4 as efficiently as cells expressing N11A when the target cells co-expressed CD4. These results suggest that the interaction of gp120 with CD4 counteracts the glycan-mediated inhibition.

To confirm this conclusion, we examined if preincubation of 8X vector particles with soluble CD4 (sCD4) could affect the glycan-mediated inhibition. The preincubation of sCD4 (20 μg ml^{-1}) enhanced transduction efficiency of the 8X vector approximately 3-fold in U87 cells expressing wt CXCR4 (Fig. 2d), as reported previously (Schenten *et al.*, 1999). In the absence of sCD4, the transduction titre in cells expressing N11A was about 5.5-fold higher than in cells expressing wt, but in the presence of sCD4, this difference was only 2.5-fold. This result indicates that sCD4 partially cancels the glycan-mediated inhibition of 8X virus infection, supporting the contention that CD4-gp120 interaction counteracts the glycan-mediated inhibition. The sCD4 treatment had lower efficiency to enhance the 8X vector infectivity and to counteract the glycan-mediated inhibition than the surface expression of CD4 on target cells. This may result from the dissociation of Env proteins from virus particles that is induced by the sCD4 treatment (Moore *et al.*, 1990; Hart *et al.*, 1991).

To help understand the molecular mechanisms by which the CXCR4 glycan affects the vector infectivity, we have built a three-dimensional (3D) model of CXCR4 with the carbohydrate moiety at the N terminus (Ponder & Case, 2003) (Fig. 3a). The crystal structure of the bovine rhodopsin [PDB code: 1F88 at 2.80 Å (0.28 nm) resolution] (Palczewski *et al.*, 2000) was used as a template for the homology modelling of CXCR4. The high-mannose carbohydrate structure was used as the N-glycan, so that we could examine minimum effects of steric hindrance against ligand access.

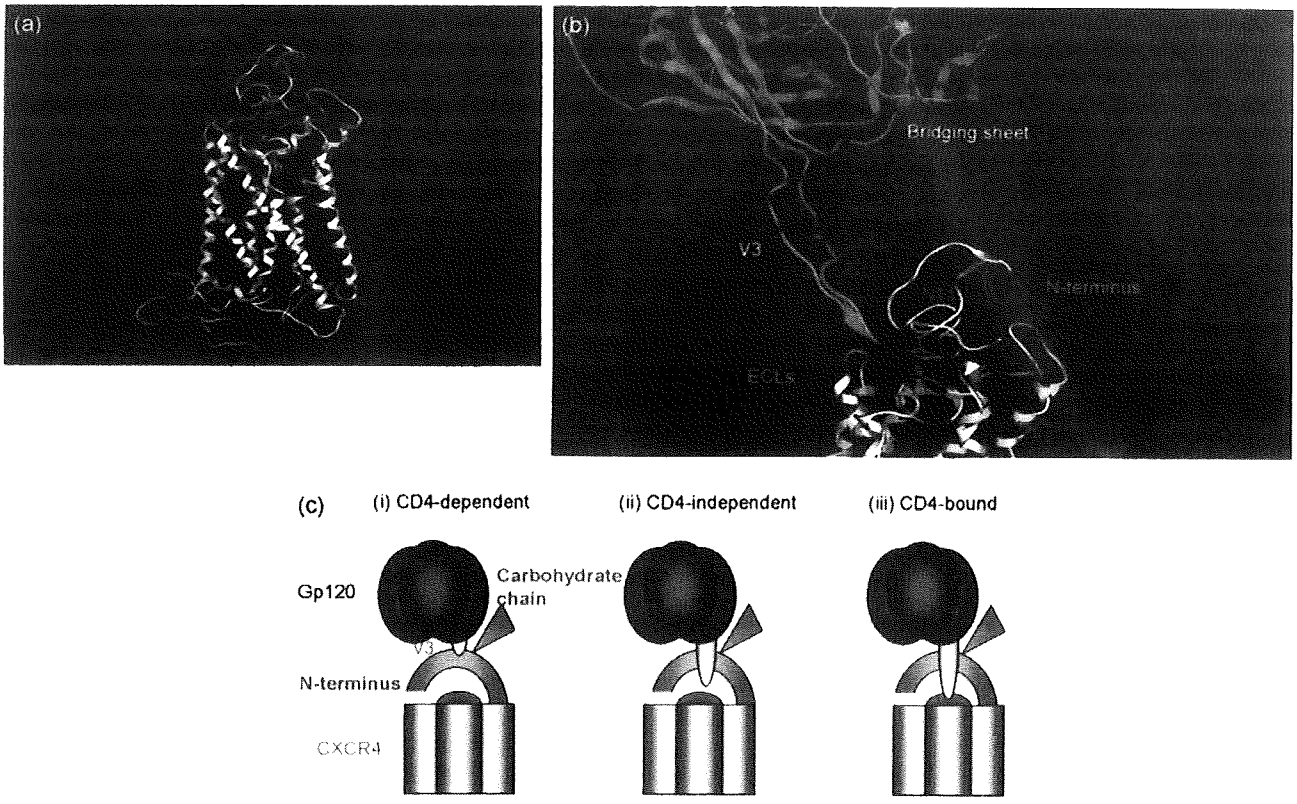

Fig. 3. Structural model of glycosylated CXCR4 and a schematic illustration of interactions between gp120 and CXCR4 during CD4-dependent and -independent infections. (a) The 3D structure of CXCR4 was constructed by homology modelling using the crystal structure of bovine rhodopsin. (b) Gp120 core with V3 (cyan, PDB code: 2B4C) was placed near the extracellular loops of the CXCR4 model (white). The purple residue indicates the glycosylated Asn. Red, blue and green residues indicate acidic, basic and uncharged polar amino acids, respectively. (c) Schematic illustration of a model of interactions between gp120 and CXCR4 during CD4-dependent and -independent infections. (i) Before CD4 binding, the V3 can rarely interact with CXCR4 due to low exposure of the CXCR4-binding moiety. (ii) After conformational change of gp120 upon binding to CD4, the V3 tip can reach the binding sites on CXCR4 due to the high level of V3 exposure. (iii) In case of the CD4-independent infection, V3 exposure is constitutive but partial, which increases sensitivity to the steric hindrance of the glycan.

Ramachandran plot, χ plot and energy minimization with AMBER-99 force field showed that the 3D model was physically and thermodynamically favoured and that it also preserves the physico-chemical features of the CXCR4 structure that were reported previously (Huang *et al.*, 2003). These features include high levels of negative electrostatic potential along the top of the extracellular surface region of CXCR4 (Fig. 3a, red residues). The negative amino acids are located on the N-terminal end and extracellular loops (ECL) 1, 2 and 3, and some of them are indicated to play important roles in binding to gp120 (Brelot *et al.*, 1997, 2000; Chabot *et al.*, 1999; Doranz *et al.*, 1999; Kajumo *et al.*, 2000; Zhou *et al.*, 2001). The 3D model suggests that these residues can function as attracting force via Coulombic interactions in the gp120 binding. In addition, the model shows that the glycan at the N terminus protrudes over this negatively charged region, narrowing space for HIV-1 Env protein access.

We found that X4 virus infectivity increased 1.5 to 5.5-fold when the virus infected human cells expressing N11A. Such an increase can be achieved by two mechanisms. First, N11A might have induced a conformation for increased binding to gp120. However, this possibility is unlikely because *in silico* structural analysis of the unglycosylated CXCR4 was nearly identical to the glycosylated counterpart. Furthermore, it is difficult to explain our results of the CD4-co-expression experiments by this mechanism. Our CXCR4 structural model supports the steric hindrance mechanism by predicting that the glycan will narrow the entry space of gp120 V3 (Fig. 3b). Unfortunately, a binding assay (Kinomoto *et al.*, 2005) did not show higher levels of 8X vector binding to N11A-expressing cells compared with wt-expressing cells (Supplementary Figure S4, available with the online version of this paper), due to the lower sensitivity of the binding assay than the vector transduction assay.

Our findings have implications for the importance of the CD4-dependent infection. CD4-independent variants are attenuated variants that are sensitive to antibody neutralization and that exist in nature only as a minor variant. CD4-dependency seems to have evolved to protect from neutralization antibodies (Bhattacharya *et al.*, 2003; Edwards *et al.*, 2001; Hoffman *et al.*, 1999; Kolchinsky *et al.*, 2001; Puffer *et al.*, 2002; Thomas *et al.*, 2003). Our data suggest that the CD4-dependent infection confers additional selective advantage other than a better defence capability. CD4-dependent viral infection was about 100-fold more efficient than CD4-independent infection. In addition, the glycan-mediated block of infection was counteracted by CD4-dependent infection. These data indicate that the CD4-independent X4 virus gains much better infectivity of human cells by CD4-mediated entry. Thus, CD4-dependent viruses dominate in nature possibly because they have a better defence capability against host immune restriction and better infectivity.

On the basis of our data and those of others, we suggest a model for the interactions between gp120 and CXCR4 upon CD4-mediated and -independent infections. Before the virus binds to CD4, the V3 loop in gp120 is less exposed (Zhu *et al.*, 2006) [Fig. 3c(i)]. Upon viral binding to CD4, massive conformational changes in gp120 induce full exposure of V3 (Huang *et al.*, 2005) [Fig. 3c(iii)] so that glycan-mediated inhibition is less efficient, leading to increase in viral infectivity, as seen in this and other studies (Brelot *et al.*, 2000; Chabot *et al.*, 2000; Picard *et al.*, 1997; Thordsen *et al.*, 2002). In the case of CD4-independent infection, however, V3 is constitutively but partially exposed (Edinger *et al.*, 1999; Edwards *et al.*, 2001; Hoffman *et al.*, 2000; Martin *et al.*, 1997), which increases sensitivity to the glycan effect [Fig. 3c(ii)]. This in turn decreases infectivity in cells expressing glycosylated CXCR4 (Potempa *et al.*, 1997; Wang *et al.*, 2004). Further biochemical studies including structure–function analysis of gp120 and receptors will help in our understanding of how the glycan on the infection receptor affect HIV infection.

Acknowledgements

We thank Dr D. Trono for the HIV-1 packaging construct (R8.91), Drs U. Hazan, R. Doms and Y. Yokomaku for the Env expression plasmids, Dr H. Hoshino for NP2 and U87 cells, and Dr K. Tokunaga for technical advice on the binding assay. The VSV-G expression plasmid and the LacZ-containing HIV-1 vector DNA were provided by Dr L. Chang through the AIDS Research and Reference Reagent Program, Division of AIDS, NIAID, NIH, USA. The sCD4 was also obtained from the above program. This work was supported by a Health Science Research Grant from the Ministry of Health, Labour and Welfare of Japan, and by the 21st century Centers of Excellence (COE) program.

References

Berger, E. A., Doms, R. W., Fenyo, E. M., Korber, B. T., Littman, D. R., Moore, J. P., Sattentau, Q. J., Schuitemaker, H., Sodroski, J. & Weiss, R. A. (1998). A new classification for HIV-1. *Nature* **391**, 240.

Bhattacharya, J., Peters, P. J. & Clapham, P. R. (2003). CD4-independent infection of HIV and SIV: implications for envelope conformation and cell tropism in vivo. *AIDS* **17** (*Suppl. 4*), S35–S43.

Brelot, A., Heveker, N., Pleskoff, O., Sol, N. & Alizon, M. (1997). Role of the first and third extracellular domains of CXCR-4 in human immunodeficiency virus coreceptor activity. *J Virol* **71**, 4744–4751.

Brelot, A., Heveker, N., Montes, M. & Alizon, M. (2000). Identification of residues of CXCR4 critical for human immunodeficiency virus coreceptor and chemokine receptor activities. *J Biol Chem* **275**, 23736–23744.

Chabot, D. J. & Broder, C. C. (2000). Substitutions in a homologous region of extracellular loop 2 of CXCR4 and CCR5 alter coreceptor activities for HIV-1 membrane fusion and virus entry. *J Biol Chem* **275**, 23774–23782.

Chabot, D. J., Zhang, P. F., Quinnan, G. V. & Broder, C. C. (1999). Mutagenesis of CXCR4 identifies important domains for human immunodeficiency virus type 1 X4 isolate envelope-mediated membrane fusion and virus entry and reveals cryptic coreceptor activity for R5 isolates. *J Virol* **73**, 6598–6609.

Chabot, D. J., Chen, H., Dimitrov, D. S. & Broder, C. C. (2000). N-linked glycosylation of CXCR4 masks coreceptor function for CCR5-dependent human immunodeficiency virus type 1 isolates. *J Virol* **74**, 4404–4413.

Chang, L. J., Urlacher, V., Iwakuma, T., Cui, Y. & Zucali, J. (1999). Efficacy and safety analyses of a recombinant human immunodeficiency virus type 1 derived vector system. *Gene Ther* **6**, 715–728.

Dimitrov, D. S. (1997). How do viruses enter cells? The HIV coreceptors teach us a lesson of complexity. *Cell* **91**, 721–730.

Doranz, B. J., Orsini, M. J., Turner, J. D., Hoffman, T. L., Berson, J. F., Hoxie, J. A., Peiper, S. C., Brass, L. F. & Doms, R. W. (1999). Identification of CXCR4 domains that support coreceptor and chemokine receptor functions. *J Virol* **73**, 2752–2761.

Dumonceaux, J., Nisole, S., Chanel, C., Quivet, L., Amara, A., Baleux, F., Briand, P. & Hazan, U. (1998). Spontaneous mutations in the env gene of the human immunodeficiency virus type 1 NDK isolate are associated with a CD4-independent entry phenotype. *J Virol* **72**, 512–519.

Edinger, A. L., Blanpain, C., Kunstman, K. J., Wolinsky, S. M., Parmentier, M. & Doms, R. W. (1999). Functional dissection of CCR5 coreceptor function through the use of CD4-independent simian immunodeficiency virus strains. *J Virol* **73**, 4062–4073.

Edwards, T. G., Hoffman, T. L., Baribaud, F., Wyss, S., LaBranche, C. C., Romano, J., Adkinson, J., Sharron, M., Hoxie, J. A. & Doms, R. W. (2001). Relationships between CD4 independence, neutralization sensitivity, and exposure of a CD4-induced epitope in a human immunodeficiency virus type 1 envelope protein. *J Virol* **75**, 5230–5239.

Hart, T. K., Kirsh, R., Ellens, H., Sweet, R. W., Lambert, D. M., Petteway, S. R., Jr, Leary, J. & Bugelski, P. J. (1991). Binding of soluble CD4 proteins to human immunodeficiency virus type 1 and infected cells induces release of envelope glycoprotein gp120. *Proc Natl Acad Sci U S A* **88**, 2189–2193.

Hoffman, T. L., LaBranche, C. C., Zhang, W., Canziani, G., Robinson, J., Chaiken, I., Hoxie, J. A. & Doms, R. W. (1999). Stable exposure of the coreceptor-binding site in a CD4-independent HIV-1 envelope protein. *Proc Natl Acad Sci U S A* **96**, 6359–6364.

Hoffman, T. L., Canziani, G., Jia, L., Rucker, J. & Doms, R. W. (2000). A biosensor assay for studying ligand-membrane receptor interactions: binding of antibodies and HIV-1 Env to chemokine receptors. *Proc Natl Acad Sci U S A* **97**, 11215–11220.

Huang, X., Shen, J., Cui, M., Shen, L., Luo, X., Ling, K., Pei, G., Jiang, H. & Chen, K. (2003). Molecular dynamics simulations on SDF-1alpha: binding with CXCR4 receptor. *Biophys J* **84**, 171–184.

Huang, C. C., Tang, M., Zhang, M. Y., Majeed, S., Montabana, E., Stanfield, R. L., Dimitrov, D. S., Korber, B., Sodroski, J. & other authors (2005). Structure of a V3-containing HIV-1 gp120 core. *Science* **310**, 1025–1028.

Iwakuma, T., Cui, Y. & Chang, L. J. (1999). Self-inactivating lentiviral vectors with U3 and U5 modifications. *Virology* **261**, 120–132.

Kajumo, F., Thompson, D. A., Guo, Y. & Dragic, T. (2000). Entry of R5X4 and X4 human immunodeficiency virus type 1 strains is mediated by negatively charged and tyrosine residues in the amino-terminal domain and the second extracellular loop of CXCR4. *Virology* **271**, 240–247.

Kinomoto, M., Yokoyama, M., Sato, H., Kojima, A., Kurata, T., Ikuta, K., Sata, T. & Tokunaga, K. (2005). Amino acid 36 in the human immunodeficiency virus type 1 gp41 ectodomain controls fusogenic activity: implications for the molecular mechanism of viral escape from a fusion inhibitor. *J Virol* **79**, 5996–6004.

Kolchinsky, P., Kiprilov, E. & Sodroski, J. (2001). Increased neutralization sensitivity of CD4-independent human immunodeficiency virus variants. *J Virol* **75**, 2041–2050.

Kubo, Y., Ono, T., Ogura, M., Ishimoto, A. & Amanuma, H. (2002). A glycosylation-defective variant of the ecotropic murine retrovirus receptor is expressed in rat XC cells. *Virology* **303**, 338–344.

Kubo, Y., Ishimoto, A. & Amanuma, H. (2003). N-Linked glycosylation is required for XC cell-specific syncytium formation by the R peptide-containing envelope protein of ecotropic murine leukemia viruses. *J Virol* **77**, 7510–7516.

Kubo, Y., Ishimoto, A., Ono, T., Yoshii, H., Tominaga, C., Mitani, C., Amanuma, H. & Yamamoto, N. (2004). Determinant for the inhibition of ecotropic murine leukemia virus infection by N-linked glycosylation of the rat receptor. *Virology* **330**, 82–91.

Marin, M., Lavillette, D., Kelly, S. M. & Kabat, D. (2003). N-linked glycosylation and sequence changes in a critical negative control region of the ASCT1 and ASCT2 neutral amino acid transporters determine their retroviral receptor functions. *J Virol* **77**, 2936–2945.

Martin, K. A., Wyatt, R., Farzan, M., Choe, H., Marcon, L., Desjardins, E., Robinson, J., Sodroski, J., Gerard, C. & Gerard, N. P. (1997). CD4-independent binding of SIV gp120 to rhesus CCR5. *Science* **278**, 1470–1473.

Moore, J. P., McKeating, J. A., Weiss, R. A. & Sattentau, Q. J. (1990). Dissociation of gp120 from HIV-1 virions induced by soluble CD4. *Science* **250**, 1139–1142.

Naldini, L., Blomer, U., Gallay, P., Ory, D., Mulligan, R., Gage, F. H., Verma, I. M. & Trono, D. (1996). In vivo gene delivery and stable transduction of nondividing cells by a lentiviral vector. *Science* **272**, 263–267.

Overbaugh, J., Miller, A. D. & Eiden, M. V. (2001). Receptors and entry cofactors for retroviruses include single and multiple transmembrane-spanning proteins as well as newly described glycophosphatidylinositol-anchored and secreted proteins. *Microbiol Mol Biol Rev* **65**, 371–389 (table of contents).

Palczewski, K., Kumasaka, T., Hori, T., Behnke, C. A., Motoshima, H., Fox, B. A., Le Trong, I., Teller, D. C., Okada, T. & other authors (2000). Crystal structure of rhodopsin: A G protein-coupled receptor. *Science* **289**, 739–745.

Picard, L., Wilkinson, D. A., McKnight, A., Gray, P. W., Hoxie, J. A., Clapham, P. R. & Weiss, R. A. (1997). Role of the amino-terminal extracellular domain of CXCR-4 in human immunodeficiency virus type 1 entry. *Virology* **231**, 105–111.

Ponder, J. W. & Case, D. A. (2003). Force fields for protein simulations. *Adv Protein Chem* **66**, 27–85.

Potempa, S., Picard, L., Reeves, J. D., Wilkinson, D., Weiss, R. A. & Talbot, S. J. (1997). CD4-independent infection by human immunodeficiency virus type 2 strain ROD/B: the role of the N-terminal domain of CXCR-4 in fusion and entry. *J Virol* **71**, 4419–4424.

Puffer, B. A., Pohlmann, S., Edinger, A. L., Carlin, D., Sanchez, M. D., Reitter, J., Watry, D. D., Fox, H. S., Desrosiers, R. C. & Doms, R. W. (2002). CD4 independence of simian immunodeficiency virus Envs is associated with macrophage tropism, neutralization sensitivity, and attenuated pathogenicity. *J Virol* **76**, 2595–2605.

Schenten, D., Marcon, L., Karlsson, G. B., Parolin, C., Kodama, T., Gerard, N. & Sodroski, J. (1999). Effects of soluble CD4 on simian immunodeficiency virus infection on CD4-positive and CD4-negative cells. *J Virol* **73**, 5373–5380.

Soda, Y., Shimizu, N., Jinno, A., Liu, H. Y., Kanbe, K., Kitamura, T. & Hoshino, H. (1999). Establishment of a new system for determination of coreceptor usages of HIV based on the human glioma NP-2 cell line. *Biochem Biophys Res Commun* **258**, 313–321.

Sommerfelt, M. A. (1999). Retrovirus receptors. *J Gen Virol* **80**, 3049–3064.

Tailor, C. S., Nouri, A. & Kabat, D. (2000). Cellular and species resistance to murine amphotropic, gibbon ape, and feline subgroup C leukemia viruses is strongly influenced by receptor expression levels and by receptor masking mechanisms. *J Virol* **74**, 9797–9801.

Tanaka, R., Yoshida, A., Murakami, T., Baba, E., Lichtenfeld, J., Omori, T., Kimura, T., Tsurutani, N., Fujii, N. & other authors (2001). Unique monoclonal antibody recognizing the third extracellular loop of CXCR4 induces lymphocyte agglutination and enhances human immunodeficiency virus type 1-mediated syncytium formation and productive infection. *J Virol* **75**, 11534–11543.

Thomas, E. R., Shotton, C., Weiss, R. A., Clapham, P. R. & McKnight, A. (2003). CD4-dependent and CD4-independent HIV-2: consequences for neutralization. *AIDS* **17**, 291–300.

Thordsen, I., Polzer, S. & Schreiber, M. (2002). Infection of cells expressing CXCR4 mutants lacking N-glycosylation at the N-terminal extracellular domain is enhanced for R5X4-dualtropic human immunodeficiency virus type-1. *BMC Infect Dis* **2**, 31.

Wang, J., Babcock, G. J., Choe, H., Farzan, M., Sodroski, J. & Gabuzda, D. (2004). N-linked glycosylation in the CXCR4 N-terminus inhibits binding to HIV-1 envelope glycoproteins. *Virology* **324**, 140–150.

Wilson, C. A. & Eiden, M. V. (1991). Viral and cellular factors governing hamster cell infection by murine and gibbon ape leukemia viruses. *J Virol* **65**, 5975–5982.

Zhou, N., Luo, Z., Luo, J., Liu, D., Hall, J. W., Pomerantz, R. J. & Huang, Z. (2001). Structural and functional characterization of human CXCR4 as a chemokine receptor and HIV-1 co-receptor by mutagenesis and molecular modeling studies. *J Biol Chem* **276**, 42826–42833.

Zhu, P., Liu, J., Bess, J., Jr, Chertova, E., Lifson, J. D., Grise, H., Ofek, G. A., Taylor, K. A. & Roux, K. H. (2006). Distribution and three-dimensional structure of AIDS virus envelope spikes. *Nature* **441**, 847–852.

Human Immunology (2007) 68, 563-571

ELSEVIER

ASHI AMERICAN SOCIETY FOR HISTOCOMPATIBILITY & IMMUNOGENETICS www.ashi-hla.org

journal homepage: www.elsevier.com/locate/humimm

Requirements for the functional expression of OX40 ligand on human activated CD4 and CD8 T cells

Kayo Kondo[a], Kazu Okuma[a], Reiko Tanaka[a], Li Feng Zhang[a], Akira Kodama[a], Yoshiaki Takahashi[b], Naoki Yamamoto[b], Aftab A. Ansari[c], Yuetsu Tanaka[a,*]

[a] *Department of Immunology, Graduate School of Medicine, University of the Ryukyus, Okinawa, Japan*
[b] *AIDS Research Center, National Institute of Infectious Diseases, Tokyo, Japan*
[c] *Department of Pathology and Laboratory Medicine, Emory University School of Medicine, Atlanta, GA*

Received 13 February 2007; received in revised form 11 March 2007; accepted 16 March 2007

KEYWORDS:
Human OX40L;
OX40;
T cells;
TCR stimulation;
TGF- $_1$;
IL-12;
IL-4

Summary Interaction between OX40 expressed on activated T cells and its ligand (OX40L) on antigen presenting cells (APC) provides a co-stimulatory signal for T cells to promote acquired immunity. In the present study, we have examined various culture conditions for optimum OX40L expression on T cells stimulated with immobilized anti-CD3/CD28 monoclonal antibodies (mAbs). Although the day 3 primed T cells expressed minimal OX40L, after repeated stimulations both the CD4 and CD8 T cells became OX40L positive as determined by flow cytometry. Interleukin (IL)-12 interfered with the OX40L expression. Among activated T cells, a higher frequency of CD8 T cells expressed OX40L than CD4 T cells. By blocking OX40L-OX40 interaction by an anti-OX40 mAb, the number of OX40L T cells significantly increased. Screening of various cytokines showed that transforming growth factor (TGF)- $_1$ was capable of induction of OX40L on the activated T cells within 3 days. The OX40L expressed on T cells was functional, as they bound soluble OX40 and stimulated human immunodeficiency virus-1 (HIV-1) production from cell lines chronically infected with HIV-1 and expressing OX40. Altogether the present study findings indicate that functional OX40L is inducible on human activated CD4 and CD8 T cells, and that the expression is enhanced by TGF- $_1$.

Introduction

OX40/OX40L (CD134/CD252) represent a growing number of pairs of co-stimulatory molecules and ligands that have been reported to be critical for T-cell proliferation, survival, cytokine production, and the generation of memory T cells [1-5]. The OX40/OX40L are members of the tumor necrosis factor receptor (TNFR)-TNF super-family with OX40 being transiently expressed primarily by activated T cells after ligation of the T-cell receptor (TCR). Its cognate ligand OX40L (also termed gp34) [6,7] has a broad tissue distribution (including dendritic cells, Langerhans cells, B cells, natural killer cells, vascular endothelial cells, and mast cells) and is not normally detectable on resting cells but can be upregulated after activation [8-23]. The pathophysiologic

* Corresponding author. Fax: 81-98-895-1437.
E-mail address: yuetsu@s4.dion.ne.jp (Y. Tanaka).

0198-8859/$ -see front matter © 2007 American Society for Histocompatibility and Immunogenetics. Published by Elsevier Inc. All rights reserved.
doi:10.1016/j.humimm.2007.03.012

ABBREVIATIONS

APCs	antigen-presenting cells
HIV	human immunodeficiency virus
mAb	monoclonal antibody
OX40L	OX40 ligand
PBMCs	peripheral blood mononuclear cells
TCR	T-cell receptor
TGF	transforming growth factor
TNF	tumor necrosis factor
TNFR	tumor necrosis factor receptor
FCM	flow cytometry

relevance of such broad tissue distribution of OX40L requires further study. The interaction between OX40 and OX40L has been described as being highly plastic, a characteristic of the TNFR-TNF super-family that was recently confirmed by the delineation of the crystal structure of the OX40/OX40L complex [24].

Although initially the expression of OX40L was thought to be restricted to non-T cells, recent studies appear to question this view. Thus it has been shown that OX40L is in fact inducible on long-term cultured human CD4 and CD8 cytotoxic T-cell lines in addition to T-cell lines transformed by human T-cell leukemia virus type I (HTLV-I) [16,25,26]. In the murine system it has been reported that functional OX40L can be induced on TCR-transgenic T cells when they are stimulated *in vitro* [27,28]. More recently the data from Soroosh *et al.* [29] suggested that indeed OX40L expressed by murine T cells participates in an unique T-T-cell signaling system by interaction with OX40 and that such interactions are critical for long-term survival of such T cells. Although these studies have been performed using murine T cells, a role for such T-T-cell interaction, along with the optimum conditions and requirements for OX40L expression by human T cells, have yet to be defined. Thus the present studies were conducted to define first the culture conditions that promote OX40L expression by human T cells *in vitro*. We show here that activated human CD4 and CD8 T cells both can express functional OX40L *in vitro* specially after repeated stimulation, and that TGF- 1 is a strong inducer of OX40L. The role of OX40L expressed by T cells is discussed.

Subjects and methods

Reagents

Medium used was RPMI-1640 medium (Sigma, St. Louis, MO) supplemented with 5% heat-inactivated fetal calf serum (FCS) (Sigma) (referred to as RPMI medium). No antibiotics were added. Recombinant human IL-2 (rIL-2) was provided courtesy of the US National Institutes of Health AIDS Research and Reference Reagent Program. The recombinant cytokines rIL-12, rIL-4, rIL-10, rIL-17, rIL-18 rIFN- , and rTGF- $_1$ were purchased from Peprotec (London, UK). The fluorescent mAbs specific for human CD4 and CD8 (PE or PC5-labeled) and Streptavidin-PE were purchased from Beckman-Coulter (Fullerton, CA). The mAbs produced in our laboratory included mouse IgG1 anti-OX40L (clone 5A8) [30], rat IgG2b anti-HCV (clone Mo-8) [31], mouse IgG1 anti-human OX40 (clone B-7B5) [32], rat IgG2b anti-OX40 (clone W4-54 which was generated from a WKA rat and capable of blocking OX40/OX40L interaction), and control mouse IgG1 mAb TAXY-8 anti-HTLV-I tax antigen [33]. The mAbs from clones B-7B5 and W4-54 recognized different epitopes of OX40 and did not interfere with each other in terms of binding to the same molecule (unpublished data). These in-house mAbs were purified from SCID mouse ascites fluids by gel filtration using Superdex G-200 (Amersham Bioscience, Uppsala, Sweden). These mAbs were labeled using FITC- or Cy5-labeling kits (Dojin, Tokyo, Japan or Amersham) according to the manufacture's instructions. Human T-cell-negative isolation kit, magnetic beads conjugated with anti-human CD3 and anti-human CD28 mAbs, and magnetic beads conjugated with anti-human CD4 or CD8 were all purchased from Dynal Corporation (Oslo, Norway). Biotinylated recombinant soluble human OX40 (sOX40, CD134-mulgG2a/biotin fusion protein) and OX40L (sOX40L, CD134L-muCD8/biotin) were purchased from Ancell (Bayport, MN). A control for mouse IgG2a was purchased from Ancell. Neutralizing mAbs specific for human TNF- and TNF- were purchased from R&D (Minneapolis, MN). Anti-CD28 mAb with stimulating activity was purchased from R&D.

Cell lines

An ACH-2 cell line chronically infected with HIV-1 and expressing OX40 was derived by OX40-gene transfection as described previously [32]. Other OX40-, OX40L- and control-gene transfected cell lines used in the present study were generated from the human T-cell line Molt-4 expressing human CCR5 (kindly provided by Dr. M. Baba of Kagoshima University, Japan), and the human promonocytic cell line U1, which was derived from the HIV-1-chronically infected U937 cell line. These cell lines were transfected by electroporation using 10-15 g of the individual plasmid, as described previously [32]. For the selection of transfectants, 1 g/ml puromycin was added to the culture media. The expression of the OX40L or OX40 protein on the cell surface of the transfected cells was confirmed by an immuofluorescence followed by flow cytometry (FCM).

Stimulation of T cells *in vitro*

Human peripheral blood mononuclear cells (PBMCs) were isolated from heparinized (5 U/ml) blood of normal healthy donors using standard density gradient centrifugation with the use of the human lymphocyte separation medium (Sigma). The cells at the interface were collected and washed three times in cold phosphate-buffered saline (PBS) containing 0.1% bovine serum albumin. The PBMCs were resuspended at 1 10^6 cells/ml in RPMI medium supplemented with 20 U/ml IL-2. Then 1 ml of the cell suspension was dispensed into individual wells of 12-well plates (B-D, NJ, USA) and mixed with the anti-CD3/CD28 magnetic beads (anti-CD3/28 immunobeads) at a cell to bead ratio of 1:1, and cultured either in the presence or absence of exogenous IL-12, IL-4 or other recombinant cytokines at 20 ng/ml for 3 days at 37° C in a 5% CO_2-humidified incubator. In some

experiments, PBMCs were stimulated by plate bound OKT-3 (0.05, 0.5, or 5 g/ml) and soluble anti-CD28 mAb (1 g/ml). In addition, for some experiments, T cells were purified using a human CD3 T-cell-negative isolation kit. Viable cell numbers were assessed on an aliquot of such cells utilizing staining with 0.1% eosin-Y in PBS. After 3 days, activated cells were harvested, adjusted to 2 10^5 cells/ml and further stimulated using the same conditions every 3 days. The anti-OX40 blocking mAb (W4-54) or control mAb (Mo-8) was added to T-cell stimulation cultures at 5 g/ml.

Flow cytometry

Cells to be analyzed were incubated in a FACS buffer (PBS containing 0.1% NaN_3 and 2% FCS) containing 2 mg/ml human IgG on ice for 15 minutes for the blocking of Fc receptors. Without washing, the cells were then subjected to staining with a set of dye-conjugated mAbs, 5A8-FITC and B-7B5-Cy5, with either anti-CD4-PE or anti-CD8-PE on ice for 30 minutes. Then after washing with FACS buffer, cells were fixed in 1% PFA-containing FACS buffer and analyzed using FACS-Calibur, and data obtained were analyzed using Cell Quest software (BD, Bedford, MA). In order to determine whether activated T cells can bind OX40L and OX40, Fc-blocked cells were incubated with biotinylated sOX40 or sOX40L at 2.5 g/ml together with either anti-CD4-PC5 or CD8-PC5 for 30 minutes on ice followed by staining with PE-labeled streptavidin (Beckman Coulter) for 30 minutes on ice. After washing with FACS buffer, cells were fixed in 1% PFA-containing FACS buffer and analyzed. In the experiments that were conducted to demonstrate the ability of W4-54 mAb to block the transfer of OX40 to OX40L and vice versa, aliquots of the Molt4/OX40L cells were mixed with Molt4/OX40 cells in the presence of 5 g/ml W4-54 or control rat IgG for 30 minutes on ice. These cell aliquots were then incubated with predetermined optimum concentrations of the 5A8-FITC and B-7B5-Cy5 mAb and subjected to flow-cytometric analysis.

OX40 stimulation assay

Two HIV-1-chronically infected cell lines (ACH-2 and U1) that had been transfected with human OX40 gene (ACH-2/OX40 and U1/OX40) ([32] and Takahashi *et al.*, unpublished data) were suspended at 2 10^5 cells/ml and co-cultured with equal number of previously activated T cells in a volume of 0.5 ml in a 48-well plate (BD) in RPMI medium for 24-48 hours at 37° C in a 5% CO_2 humidified incubator. To neutralize endogenous TNF, anti-human TNF- and TNF- mAbs (at 5 g/ml each) were included to block the potential effects of these cytokines synthesized endogenously. HIV-1 replication was determined by quantification of HIV-1 core p24 antigen in the supernatant fluid from such cultures utilizing commercial ELISA kits (Zeptometrix Corp., Buffalo, NY).

Results

Induction of OX40L on human T cells by repeated stimulation

Results from a series of preliminary studies carried out confirmed previous observations that the expression of both

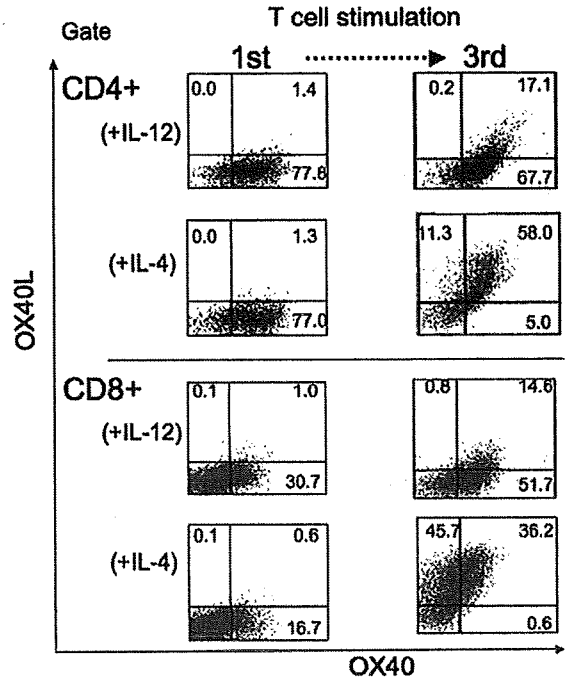

Figure 1. OX40L expression by human activated T cells. Peripheral blood mononuclear cells (PBMCs) were stimulated with anti-CD3/CD28 immunobeads in the presence of interleukin (IL)-2 together with either IL-12 (IL-12) or IL-4 (IL-4) every 3 days. T cells 3 days after the first stimulation (1st) and third stimulation (3rd) were subjected to a multicolor staining using 5A8-FITC, B-7B5-Cy5 and either CD4-PE or CD8-PE. Flow-cytometric data on OX40L and OX40 expression by T cells of CD4 or CD8 gate were shown as dot blots. Numbers in the dot-plot graphs indicate percent positive cells. Data are representative of three similar experiments.

OX40L and OX40 were undetectable on resting T cells isolated from fresh human PBMCs from a number of normal donors as determined by standard FCM (data not shown). To examine the expression of OX40L and OX40 on activated human T cells, PBMCs were incubated *in vitro* with anti-CD3/28 immunobeads. Predetermined optimum concentrations of IL-2 and either IL-12 or IL-4 were added to the cultures to generate prototype Th1 or Th2-like populations of human CD4 and CD8 T cells to examine them for the expression of OX40L and OX40. After 3 days in such culture conditions, the cultures were harvested and the expression of OX40L and OX40 by the CD4 and CD8 T cells was examined by a triple-color staining method. As seen in Figure 1, although 75% of the CD4 T cells and 16-30% of the CD8 T cells expressed cell surface OX40, 1.5% of these cells expressed OX40L irrespective of the Th1 or Th2-inducing culture conditions. In efforts to determine if repeated stimulation would facilitate OX40L expression, similar cultures were set up except fresh anti-CD3/28 immunobeads and the same cytokine mixtures were added on days 3 and 6, and the cultures harvested on day 9. Such repeated stimulation had interesting results. Although IL-12 had a modest effect on OX40L expression by CD4 T cells (an increase from 1.4 to 17.3%) most of which co-expressed OX40, similar cultures incubated in IL-4 led to a dramatic increase (from 1.3% to

58.0%) in the frequency of CD4 T cells that co-expressed OX40 and OX40L. On the other hand, although similar repeated stimulation in the presence of IL-12 yielded similar effects on the co-expression of OX40L by CD8 OX40 T cells (an increase from 1% to 14.6%) as CD4 T cells, stimulation in the presence of IL-4 not only led to an increase in OX40 OX40L (double positive (DP)) cells (from 0.6% to 36.2%) but also a discrete population of CD8 T cells that expressed only OX40L (from 0.1% to 45.7%). Repeated studies performed on different days using similar culture conditions showed some degree of variability in the levels of OX40L expression depending upon the donor of the PBMCs (data not shown). However, the basic trend was the same in that whereas the inclusion of IL-12 always led to a modest increase in the frequency of OX40 OX40L (DP) cells within both the CD4 and the CD8 T-cell populations upon repeated stimulation, the inclusion of IL-4 consistently led to an increase exclusively in OX40 OX40L (DP) cells within the CD4 T-cell population and both OX40 OX40L (DP) and single OX40L (SP) cells in the CD8 T-cell population (Figure 1 and data not shown). Because previous reports using T cells from TCR transgenic mice suggested that weak TCR stimulation is more critical for OX40L expression [34], microtiter plates were coated with the OKT-3 mAb at 5, 0.5 and 0.05 g/ml for 1 hour at 37° C, and then triplicate wells were cultured with human PBMCs for 3 days. Analyses of activated T cells from these cultures, however, failed to show any detectable changes in OX40L expression by T cells (data not shown), indicating that differences exist between murine TCR transgenic cells and human bulk T cells in terms of signals required for OX40L expression.

sOX40 binding by T cells

To examine whether the OX40L molecules expressed by these activated human T cells were functional, we examined the capacity of the repeatedly activated T cells to bind sOX40 by FCM. Figure 2 shows that although sOX40 binds preferentially to the restimulated CD8 T cells but not CD4 T cells, sOX40L binds preferentially to the restimulated CD4 T cells but not CD8 T cells. In addition, although a markedly higher frequency of the IL-4-treated CD8 T cells bound sOX40 than the IL-12-treated CD8 T cells, sOX40L bound preferentially to the restimulated CD4 T cells cultured in IL-12 as compared with IL-4. These data suggest that the induced OX40L molecules were functional in terms of their ability to bind OX40, and that the patterns of the expression of functional OX40L and OX40 by activated T cells differed depending on activation conditions and whether the T cells were of the CD4 or CD8 phenotypes.

Effect of anti-OX40 blocking mAb on OX40L expression

It has previously been shown in the murine system that OX40L expression on activated T cells is downregulated by cell-to-cell contact when co-cultured with OX40-expressing cells [29]. In addition, we have shown that human OX40L as well as OX40 molecules can be intercellularly transferred, indicating that co-expression of OX40L and OX40 by a single cell or co-cultures of cells individually expressing OX40L and

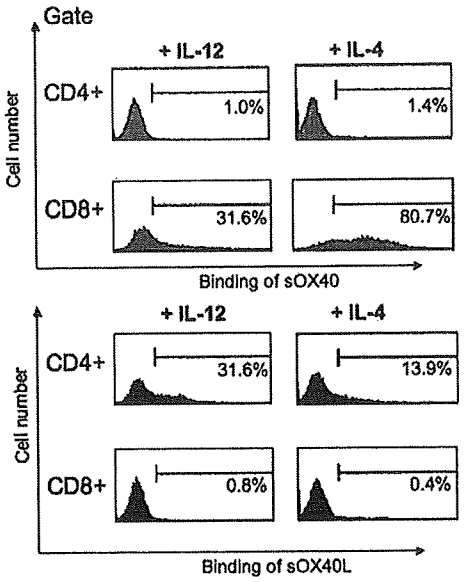

Figure 2. Expression of functional OX40L and OX40 on repeatedly activated T cells. Aliquots of cultures of peripheral blood mononuclear cells (PBMCs) restimulated three times every 3 days for a total of 9 days with anti-CD3/28 immunobeads in the presence of interleukin (IL)-2 together with either IL-12 (IL-12) or IL-4 (IL-4) were incubated with either biotinylated recombinant soluble forms of OX40 or OX40L along with either CD4-PC5 or CD8-PC5 mAb for gating. Binding of the soluble proteins was detected by using streptavidin-PE. The bars and the numbers displayed in the histogram graphs show positive area and percent positive cells. The control profile used to define the bar for the positive area was obtained on aliquots of the cultured cells untreated with the soluble proteins. Data are representative of three similar experiments.

OX40 in the same culture may interfere with OX40L expression and/or detection. To study OX40L expression without the involvement of interactions between these two molecules, a series of mAb specific for OX40 were first screened for their individual ability to block such interactions between OX40 and OX40L. A mAb clone W4-54 was thus identified that was capable of inhibiting the binding of sOX40L to membrane bound OX40. The effect of the addition of W4-54 on the binding of sOX40 to its cognate ligand OX40L was also studied. We initially used the OX40- and OX40L-transfected Molt4 cell lines for these studies in efforts to restrict the analysis to a study between these two molecules and to avoid the potential role of other cell surface molecules expressed by mixed cell populations in primary cultures. Figure 3 shows the data obtained. Thus, as seen in Figure 3a, the addition of the W4-54 mAb completely blocked the ability of sOX40L to bind to the Molt4 cell membrane-expressed OX40 (top panel). Similarly the addition of the same W4-54 mAb markedly decreased the binding of sOX40 to the Molt4 membrane bound OX40L (bottom panel). The partial blocking in this latter case may be caused by differences in the affinity of the mAb to bind to the sOX40 and the affinity of sOX40 to bind to the Molt4 membrane expressed OX40L. The ability of the W4-54 mAb to inhibit interaction between OX40 and OX40L is further exemplified by the data shown in Figure 3b.

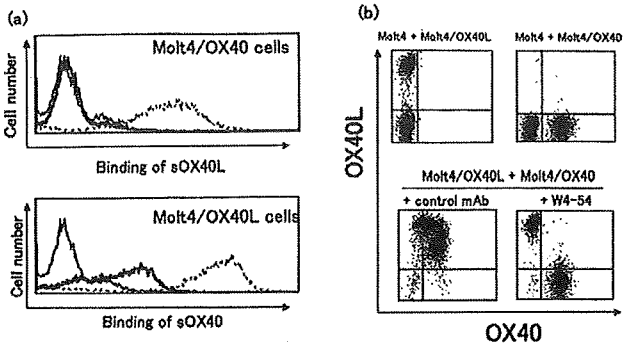

Figure 3. Anti-OX40 mAb (W4-54) blocks OX40-OX40L interaction. (a) Molt4 cells expressing OX40 (Molt4/OX40) or those expressing OX40L (Molt4/OX40L) were preincubated with 5 g/ml W4-54 or negative control mAb (Mo-8) for 30 minutes on ice. These cells were then incubated with biotinylated sOX40L or sOX40 without washing for additional 30 minutes on ice followed by staining with streptavidin-PE. Top and bottom panels depict the sOX40L binding to Molt4/OX40 cells and sOX40 binding to Molt4/OX40L cells, respectively. Thin line represents background staining with streptavidin-PE; dotted line represents staining with sOX40L or sOX40 in the presence of the negative control mAb; thick dark line represents staining in the presence of the W4-54 blocking antibody. Data shown are representative of three similar experiments. (b) To test the ability of W4-54 to prevent OX40 and OX40L transfer by cell-to-cell contact, Molt4/OX40L cells and Molt4/OX40 cells were each mixed either with the mock-transfected Molt4 cells or mixed with each other in the presence of 5 g/ml of W4-54 blocking antibody or, for purposes of control, the Mo-8 mAb on ice for 30 minutes. These mixed populations of cells were then stained with anti-OX40L-FITC (5A8) and a different clone of anti-OX40-Cy5 (B-7B5). Representative data from three experiments are shown. Note that when Molt4/OX40L cells and Molt4/OX40 cells were co-cultured in the control mAb, the Molt4/OX40 cells acquired OX40L, and at the same time, the Molt4/OX40L cells acquired OX40 as we showed previously [35].

Thus when the OX40 transfected Molt4 cells were co-cultured with the OX40L-transfected Molt4 cells and the mixed cells analyzed for OX40 and OX40L expression in the presence of the control antibody, there was significant interaction between these transfected cells (bottom left panel). However, the addition of the W4-54 mAb to the mixture of the transfected cells completely inhibited such interaction, as seen with the staining profile (bottom right panel). The top left and right panels depict the control profiles in which the OX40- and OX40L-transfected Molt4 cells were mixed with mock-transfected Molt4 cells. To determine the physiologic relevance of these findings, cultures of primary T cells were similarly examined for the expression of OX40L and OX40 after *in vitro* culture in media containing either IL-12 or IL-4 in the presence of either the same blocking W4-54 antibody or control Mo-8 mAb.

Addition of this blocking anti-OX40 mAb to the T-cell cultures stimulated by anti-CD3/28 (as described in Figure 1) did not show any significant increase in the OX40L expression after the first stimulation (Figure 4, top panel), indicating that the numbers of OX40L molecules on the T cells were few at early stage of stimulation. After the third stimulation, however, the antibody treatment showed a marked increase in the frequency of OX40L cells in both CD4 and CD8 T-cell subpopulations treated with IL-12 (Figure 4, bottom panel), indicating that the OX40L molecules detected on the activated human T cells were endogenously synthesized but not transferred from other cells. In addition, these data highlight the problems associated with the analysis of OX40 and OX40L expression on such cultured cells if performed without preventing the interactions between these two molecules either by direct cell-to-cell interaction or by the transfer of soluble forms of such molecules.

Effect of TGF- $_1$

We screened a number of recombinant human cytokines in combination with IL-2 that might influence the expression of OX40L by activated T cells. As shown in Figure 5, among the cytokines tested, only TGF- $_1$ showed a low (by CD4 T cells) to modest (by CD8 T cells) enhancement in the induction of OX40L on the activated T cells after as little as 3 days in culture *in vitro*. The cytokines that failed to induce OX40L included IL-10, IL-13, IL-17, IL-18, IFN- , and IFN- (Figure 5 and unpublished data), which was not secondary to the dose of the cytokine used. It is noteworthy that IL-12 and IL-13 also increased the frequency of CD8 T cells that express OX40. Studies carried out on primary cultures of PBMCs from another donor incubated *in vitro* in media containing TGF- $_1$ for 3 days showed that TGF- $_1$ influenced the expression of OX40L by a higher frequency of the CD8 T-cell population than the CD4 T-cell population (Figure 6a). In addition,

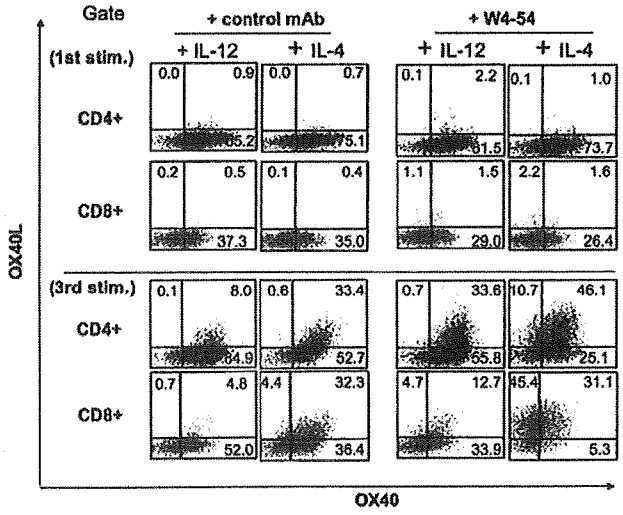

Figure 4. Effect of anti-OX40 blocking monoclonal antibody (mAb) on the expression of OX40L by T cells. Peripheral blood mononuclear cells were stimulated for 3 days (1st stim) or re-stimulated on days 3 and 6 and harvested on day 9 (3rd stim) as described in Figure 1 in the presence of either interleukin (IL)-12 or IL-4 and in the presence of either 5 g/ml W4-54 or the control mAb (Mo-8). The cells were then analyzed for the expression of OX40L and OX40 using 5A8-FITC and B-7B5-Cy5, respectively. Data reflect the profile observed on gated populations of CD4-PE-positive or CD8-PE-positive cells; data are representative of three similar experiments.

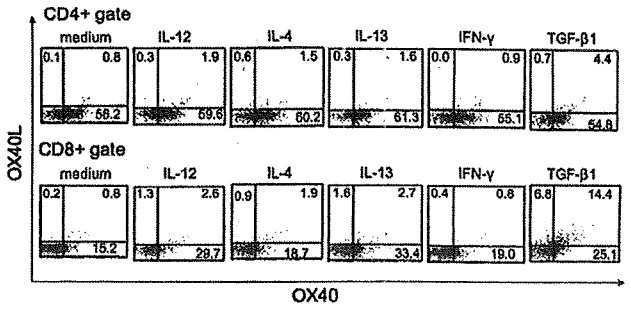

Figure 5. Effect of various cytokines on the induction of OX40L by primary activated T cells. Peripheral blood mononuclear cells were cultured *in vitro* for 3 days as described in Figure 1 in the presence of 20 U/ml interleukin (IL)-2 in combination with each of various cytokines at 20 ng/ml. Thereafter, the cells were stained with 5A8-FITC and B-7B5-Cy5 together with either CD4-PE or CD8-PE. The cells were then subjected to flow-cytometric analysis and the profile of OX40 or OX40L was determined on CD4- or CD8-gated populations of cells. Data are representative of three similar experiments.

there was a distinct population of CD8 T cells that only expressed OX40L but not OX40. To determine whether the TGF- $_1$-induced OX40L was functional, aliquots of the TGF- $_1$-induced PBMCs were incubated with biotinylated sOX40 or biotinylated sOX40L followed with streptavidin-PE. As seen in Figure 6b, OX40L expressed by the TGF- $_1$-treated CD4 and CD8 T cells was quite functional (giving values of 24.3% and 61.7% positive, respectively). However, TGF- $_1$ treatment rendered the OX40 molecules nonfunctional, as shown by a reduction of percentages of CD4 T cells bound by sOX40L from 33.2% to 3.4%. To exclude the possibility that the OX40L was passively acquired and synthesized by non-T cells in PBMCs, we stimulated purified CD3 T cells in the presence of both TGF- $_1$ and anti-OX40 blocking mAb (W4-54), and confirmed that TGF- $_1$ induced the endogenous expression of OX40L on both the CD4 and CD8 T cells as early as 12 hours (data not shown).

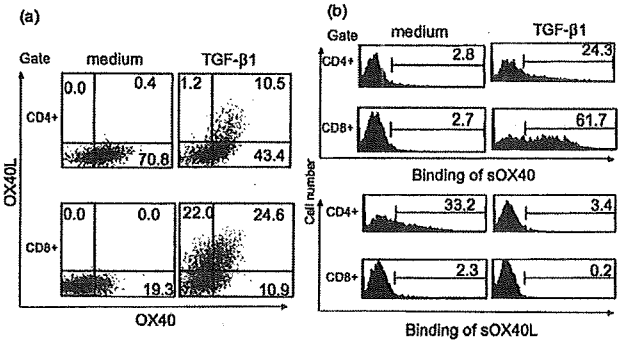

Figure 6. Transforming growth factor- $_1$ (TGF- $_1$) triggers functional OX40L expression on primary activated T cells. Peripheral blood mononuclear cells from another donor different from one examined in Figure 5 were activated (as described in Figure 1) in interleukin (IL)-2 medium either in the presence or absence of 20 ng/ml TGF- $_1$ for 3 days. (a) Expression of OX40L and OX40 was determined by a multicolor staining with mAbs as outlined in Figure 1 legend. (b) Bindings of sOX40 and sOX40L proteins were examined as described in Figure 2 legend. Data are representative of three similar experiments.

Cell-stimulating function of OX40L expressed on T cells

Finally, to confirm that the OX40L induced on the activated human T cells are biologically functional (in addition to having the potential to bind their cognate ligand), we tested whether these OX40L T cells could stimulate HIV-1 production from HIV-1-chronically infected T-cell (ACH-2) and the monocytic cell lines (U1) expressing OX40. Activation by the intracellular NF- B pathway has been shown to be the pathway by which OX40 stimulation induces HIV-1 replication in such cells [32]. Figure 7 shows that human bulk T cells repeatedly stimulated in the presence of anti-CD3/CD28 immunobeads and IL-4 as well as those stimulated once in the presence of the immunobeads, and that TGF- $_1$ could stimulate HIV-1 replication in the OX40-expressing T-cell and monocytic cell lines (Figures 7a and 7b, respectively). It is apparent that the cell activation which resulted in HIV-1 replication was mediated by OX40 stimulation by OX40L expressed on the T cells, because this induction of HIV-1 was significantly inhibited by the addition of anti-OX40L blocking mAb (clone 5A8).

Altogether the present data indicate that functional OX40L is inducible on both CD4 and CD8 *in vitro* activated human T cells, which is dependent not only on the degree of cell activation but also on the culture environment.

Discussion

The data shown here support the previous findings made by Takasawa *et al.* [25], who showed that long-term cultured cytotoxic CD4 and CD8 T-cell clones express OX40L after stimulation *in vitro*. The data reported here extend these previous findings and describe new culture conditions that lead to the induction of OX40L on human CD4 and CD8 T cells. Importantly, we demonstrated for the first time that the OX40L molecules induced on the T cells were functional, as they were capable not only of binding soluble recombinant OX40 but also of stimulating OX40-expressing cells (Figures 2 and 7). Importantly, the OX40L molecules detected on the activated T cells were endogenously synthesized, but not those transferred from other non-T cells [35], as demonstrated by using the anti-OX40 blocking mAb (W4-54) during *in vitro* activation in the cultures. Interestingly, the findings here also show for the first time that the immune-suppressive cytokine TGF- $_1$ accelerated OX40L expression by primary cultures of activated human CD4 and CD8 T cells. The data presented here also show that the stimulated individual CD4 or CD8 T-cell could co-express OX40L along with OX40.

The reason why repeated activation was necessary for high levels of OX40L expression by the human T cells *in vitro* remains to be elucidated. In the murine system, it has been reported that bulk splenic T cells from normal adult mice do not express detectable levels of OX40L after stimulation with anti-CD3 with or without anti-CD28 stimulation either [13]. This is in contrast to the murine TCR-transgenic T cells that express OX40L readily after antigenic stimulation within

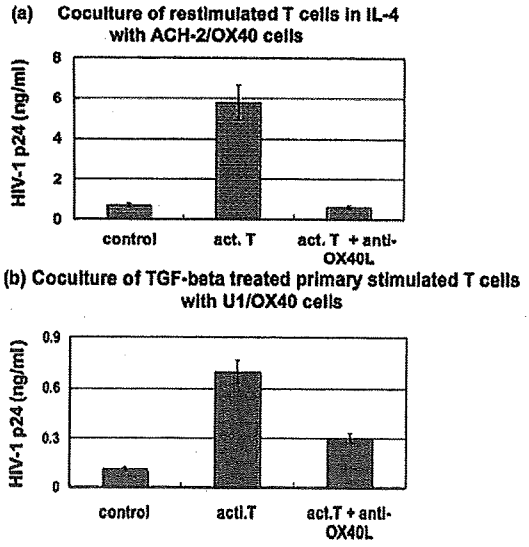

Figure 7. Effect of human T cells stimulated with anti-CD3/CD28 immunobeads either three times or once in the presence of interleukin (IL)-4 or transforming growth factor (TGF)- $_1$, respectively, on HIV-1 production from HIV-chronically infected cell lines expressing OX40. (a) ACH-2 cells expressing OX40 (ACH-2/OX40) were co-cultured for 24 hours with T cells that had been previously stimulated three times on days 0, 3, and 6 with anti-CD3/CD28 immunobeads for a total of 9 days in the presence of IL-4 and IL-2. (b) U1 cells expressing OX40 (U1/OX40) were co-cultured for 2 days with peripheral blood mononuclear cells that had been stimulated with anti-CD3/CD28 immunobeads in the presence of TGF- $_1$ and IL-2 for 3 days. Because endogenous tumor necrosis factor (TNF)- and - are capable of stimulating these two cell lines leading to HIV-1 production, 5 g/ml anti-TNF- and - were included during the culture period. Anti-OX40L mAb (5A8) at 5 g/ml was used to block OX40L-OX40 interactions. The levels of HIV-1 p24 produced in the culture supernatants were determined by enzyme-linked immunosorbent assay. Controls consisted of the ACH-2/OX40 and the U1/OX40 cells cultured alone (controls), and the ACH-2/OX40 and the U1/OX40 cells treated with anti-OX40L antibody before co-culture with the OX40L-expressing activated T cells (act.T anti-OX40L). Each combination of culture was performed in triplicate; bars indicate standard errors. Data are representative of three similar experiments.

a few days [27,29]. Thus it is likely that the expression of OX40L by bulk T cells, but not single TCR-expressing T cells, is under tight control during the initial stage of T-cell activation in normal mice and human beings. Under physiologic conditions, OX40L expression by T cells might be programmed to occur at a later stage of immune responses in order to maintain induced effector memory helper T cells [29].

Our present data suggest that the cytokine environment in the cultures in which T-cell stimulation is carried out significantly affects OX40L expression. We found that IL-12 was inhibitory for the expression of OX40L by T cells (Figures 1 and 2). Because the percentages of OX40 T cells were higher in IL-12-treated T cells than those untreated or IL-4-treated, and anti-OX40 blocking mAb reversed the inhibitory effect of IL-12 on OX40L expression (Figure 4), it seems likely that IL-12 reduced the OX40L expression by T cells through enhanced production of functional OX40 molecules. Again, the effect of IL-12 on OX40L expression by human T cells is in contrast to the murine TCR-transgenic T cells. In this mouse system, the T cells preferentially express OX40L when they are stimulated in the presence of IL-12 via the activation of the STAT-4 pathway, and IL-4 severely downmodulates OX40L expression [27,28]. Also in contrast to human cases, these TCR-transgenic T cells express enhanced levels of OX40 after treatment with IL-4. These discrepancies in OX40L and OX40 induction may be ascribed to species-specific differences or simply because of a difference in the materials tested, *i.e.*, bulk T cells from normal adults versus T cells from the TCR-transgenic mice. Experiments using naive human T cells stimulated in the presence of anti-IL-4 (Th1-rich) or bulk T cells from normal mice may provide clues to such issues.

Even though there are some discrepancies between the human and murine systems, it is now apparent that endogenous OX40L molecules can be expressed on the activated T cells. Thus, functional OX40L molecules expressed at the cell surface may immediately interact with functional OX40 molecules expressed on the same T-cell or adjacent T cells. The fate of OX40L on the T cells is unknown, and thus studies are required to address this issue in more detail in the future. It is possible that some human OX40L may be downmodulated via a post-transcriptional and cell-to-cell contact-dependent mechanisms as the murine T-cell cases as shown by Soroosh *et al.* [29]. Our present data indicate that some OX40L and OX40 molecules remained on the T-cell surface without being bound by OX40 and OX40 molecules, respectively (Figure 2). In addition, some OX40L molecules on T cells may be transferred to adjacent cells via an OX40-dependent and/or independent manner [35].

The present study also revealed that the patterns of OX40L and OX40 expression were quite different between CD4 and CD8 T-cell subpopulations. Thus, whereas the CD4 T cells tend to preferentially express OX40, the CD8 T cells appear to preferentially express OX40L (Figures 1 and 4). This difference was not merely phenotypic but also functional, because functional OX40L molecules that could bind soluble OX40 were abundant in CD8 T cells and the OX40 molecules expressed by CD4 T cells could bind sOX40L (Figure 2). One possible mechanism for this may be that the molecular ratios of OX40L and OX40 synthesized in these subpopulations are different. This phenotypic difference indicates that a communication between CD4 and CD8 T cells via OX40L-OX40 interaction is also possible. Because 0X40L-OX40 bindings have been shown to mediate cell to cell adhesion, it is highly possible that the OX40L-OX40 interaction may facilitate cross-talk between the two T-cell populations after activation. In the murine system, Soroosh *et al.* [29] hypothesized that OX40L expressed by CD4 T cells can provide autonomous OX40 signals through interactions between T cells, which contribute to the longevity of antigen-specific CD4 T cells and thus lead to the generation and survival of CD4 memory T cells. The other functions suggested in the murine sytem include deviation of a Th1 response to a Th2 response [28], and control of Th2 proliferation [27]. Another possible speculation is that in addition to the immune-stimulating roles, the OX40L/OX40 interaction